AGU PUBLICATIONS

JGR

Journal of Geophysical Research: Solid Earth

RESEARCH ARTICLE
10.1002/2015JB012123

Key Points:
- Hydration reduces K_0 of wadsleyite significantly
- Hydration does not influence dK/dP of wadsleyite
- Hydration reduces bulk sound velocity at transition zone conditions

Correspondence to:
Y.-Y. Chang,
ychang@earth.sinica.edu.tw

Citation:
Chang, Y.-Y., et al. (2015), Comparative compressibility of hydrous wadsleyite and ringwoodite: Effect of H_2O and implications for detecting water in the transition zone, *J. Geophys. Res. Solid Earth*, *120*, doi:10.1002/2015JB012123.

Received 16 APR 2015
Accepted 8 NOV 2015
Accepted article online 17 NOV 2015

Comparative compressibility of hydrous wadsleyite and ringwoodite: Effect of H_2O and implications for detecting water in the transition zone

Yun-Yuan Chang[1,2], Steven D. Jacobsen[1], Craig R. Bina[1], Sylvia-Monique Thomas[3], Joseph R. Smyth[4], Daniel J. Frost[5], Tiziana Boffa Ballaran[5], Catherine A. McCammon[5], Erik H. Hauri[6], Toru Inoue[7], Hisayoshi Yurimoto[8], Yue Meng[9], and Przemyslaw Dera[10]

[1]Department of Earth and Planetary Sciences, Northwestern University, Evanston, Illinois, USA, [2]Now at Institute of Earth Sciences, Academia Sinica, Taipei, Taiwan, [3]Department of Geoscience, University of Nevada, Las Vegas, Las Vegas, Nevada, USA, [4]Department of Geological Sciences, University of Colorado Boulder, Boulder, Colorado, USA, [5]Bayerisches Geoinstitut, University of Bayreuth, Bayreuth, Germany, [6]Department of Terrestrial Magnetism, Carnegie Institution of Washington, Washington, District of Columbia, USA, [7]Geodynamics Research Center, Ehime University, Matsuyama, Japan, [8]Department of Natural History Sciences, Hokkaido University, Sapporo, Japan, [9]High-Pressure Collaborative Access Team, Carnegie Institution of Washington, Argonne, Illinois, USA, [10]Hawaii Institute of Geophysics and Planetology, University of Hawai'i at Mānoa, Honolulu, Hawaii, USA

Abstract Review of recent mineral physics literature shows consistent trends for the influence of Fe and H_2O on the bulk modulus (K_0) of wadsleyite and ringwoodite, the major phases of Earth's mantle transition zone (410–660 km). However, there is little consensus on the first pressure derivative, $K_0' = (dK/dP)_{P=0}$, which ranges from about 4 to >5 across experimental studies and compositions. Here we demonstrate the importance of K_0' in evaluating the bulk sound velocity of the transition zone in terms of water content and provide new constraints on the effect of H_2O on K_0' for wadsleyite and ringwoodite by conducting a comparative compressibility study. In the experiment, multiple crystals of hydrous Fo_{90} wadsleyite containing 2.0 and 0.25 wt % H_2O were loaded into the same diamond anvil cell, along with hydrous ringwoodite containing 1.4 wt % H_2O. By measuring their pressure-volume evolution simultaneously up to 32 GPa, we constrain the difference in K_0' independent of the pressure scale, finding that H_2O has no effect on K_0', whereas the effect of H_2O on K_0 is significant. The fitted K_0' values of hydrous wadsleyite (0.25 and 2.0 wt % H_2O) and hydrous ringwoodite (1.4 wt % H_2O) examined in this study were found to be identical within uncertainty, with $K_0' \sim 3.7(2)$. New secondary-ion mass spectrometry measurements of the H_2O content of these and previously investigated wadsleyite samples shows the bulk modulus of wadsleyite is reduced by 7.0(5) GPa/wt % H_2O, independent of Fe content for upper mantle compositions. Because K_0' is unaffected by H_2O, the reduction of bulk sound velocity in very hydrous regions of transition zone is expected to be on the order of 1.6%, which is potentially detectible in high-resolution, regional seismology studies.

1. Introduction

Interpreting the internal structure, composition, and mineralogy of the Earth's mantle requires accurate thermoelastic properties of the major mineral phases and critically how these properties vary with pressure, temperature, and composition [*Birch*, 1952; *Duffy and Anderson*, 1989; *Li and Liebermann*, 2007; *Stixrude and Lithgow-Bertelloni*, 2005]. Characteristics of the seismic discontinuities at 410 km and 660 km bounding the mantle transition zone, including the depth to transition, transition interval, and impedance contrast, are affected by the chemical composition of major mantle minerals [*Bina and Helffrich*, 1994; *Frost*, 2003; *Irifune and Isshiki*, 1998; *Schmerr and Garnero*, 2007; *Sinogeikin et al.*, 2003]. Wadsleyite (β-Mg_2SiO_4) and ringwoodite (γ-Mg_2SiO_4) constitute ~60% of the transition zone in the pyrolite model of mantle composition [*Irifune and Ringwood*, 1987; *Ringwood and Major*, 1967]. In $(Mg,Fe)_2SiO_4$, upper mantle olivine typically contains $X_{Fe} = Fe/(Fe + Mg)$ of 0.07–0.15, making it essential to study Fe-bearing phases with well-characterized $Fe^{3+}/\Sigma Fe$ ratios. The recent discovery of 1.5 wt % H_2O in a natural, Fe-bearing ringwoodite inclusion in diamond [*Pearson et al.*, 2014] suggests that some regions of the transition zone may be near saturated in H_2O. Determining the combined influence of Fe and hydration on the elastic properties of wadsleyite and ringwoodite will therefore further constrain the chemical composition and water budget in the Earth's interior by comparison of experimental equations of state with high-resolution, regional seismic velocity profiles of the upper mantle.

The effect of Fe on the elastic properties of anhydrous wadsleyite can be evaluated by comparing previous studies on Mg- and Fe-bearing wadsleyite using static compression, ultrasonic, or optical-acoustic methods [e.g., *Hazen et al*., 2000a, 2000b; *Li and Gwanmesia*, 1996; *Li and Liebermann*, 2000; *Liu et al*., 2009; *Sawamoto et al*., 1984; *Sinogeikin et al*., 1998; *Wang et al*., 2014; *Zha et al*., 1997]. Fe increases the density of wadsleyite by about 3.5% for $X_{Fe} = 0.1$ compared with pure Mg-wadsleyite [*Li and Liebermann*, 2007] but has a negligible effect on the bulk modulus [*Wang et al*., 2014]. Although there is good agreement between studies on the bulk modulus of anhydrous Fe-bearing wadsleyite, the reported pressure derivative, $K_0' = (dK/dP)_{P=0}$, ranges from 4.1(1) [*Wang et al*., 2014] to 4.6(1) [*Li and Liebermann*, 2000] or 4.8 [*Gwanmesia et al*., 1990]. The range of experimental values for K_0' of wadsleyite is around 5 times the reported experimental uncertainties.

H_2O is another important geochemical variable in mantle composition. Wadsleyite incorporates water as hydroxyl $(OH)^-$ defects into its structure due to the underbonded, nonsilicate oxygen (O1) [*Smyth*, 1987, 1994], with up to ~3 wt % H_2O reported in synthetic samples [*Bolfan-Casanova et al*., 2000; *Demouchy et al*., 2005; *Inoue et al*., 1995; *Kohlstedt et al*., 1996]. Due to coupled substitutions with Mg-Fe vacancies on the M3 site [*Jacobsen et al*., 2005; *Deon et al*., 2010; *Griffin et al*., 2013], the incorporation of hydroxyl in the wadsleyite structure has significant effect on its elastic properties. Previous studies on Mg-wadsleyite show that its bulk modulus decreases by ~12 GPa per wt % H_2O added [*Holl et al*., 2008; *Mao et al*., 2008, 2011; *Ye et al*., 2010], which is also in accordance with theoretical studies [*Tsuchiya and Tsuchiya*, 2009; *Liu et al*., 2012]. Whereas previous studies of the bulk modulus have investigated either hydrous Mg-wadsleyite or anhydrous Fe-bearing wadsleyite, the combined influence of hydration and iron on the elasticity of wadsleyite at high pressure has been reported in only one experimental study thus far [*Mao et al*., 2011], who found the effects of Fe and H_2O on the bulk and shear moduli are linearly additive and reported $K_0' = 4.8(1)$ for $X_{Fe} = 0.10$ hydrous wadsleyite containing about 2 wt % H_2O. The hydrous Fe-bearing wadsleyite sample from the study of *Mao et al*. [2011] is also used in the current study for comparison with low-H_2O, Fe-bearing wadsleyite. A recent theoretical study [*Tian et al*., 2012] on the elasticity of hydrous Fe-bearing wadsleyite predicted that the incorporation of 1.6 wt % H_2O into Fe-bearing wadsleyite ($X_{Fe} = 0.125$) elevates K_0' from 3.92 to 4.12.

Whereas the effect of hydration on the bulk modulus of hydrous wadsleyite and ringwoodite is generally well constrained at room pressure and room temperature [e.g., *Jacobsen*, 2006], the influence of H_2O on K_0' is poorly constrained when considering the range of reported values cited in the literature. The pressure derivative of K is critical for estimating the effect of H_2O on the density and sound velocities of wadsleyite at transition zone pressures. The influence of hydration on the pressure derivative of the bulk modulus for wadsleyite and ringwoodite may not be well constrained for various reasons, including limited data resolution at high pressure, the use of different pressure calibrations, nonhydrostatic stresses on the sample, different data analysis methods, or the narrow pressure ranges over which data have been measured. Reported values of the bulk modulus of anhydrous Mg-wadsleyite (Fo_{100}) are in good agreement with K_0 ~170 GPa; however, values of K_0' range from 4.2 to 6.3 [e.g., *Holl et al*., 2008; *Hazen et al*., 2000a; *Li and Gwanmesia*, 1996; *Zha et al*., 1997]. Figure 1 summarizes the K_0' values of wadsleyite from published experimental studies. The values of K_0' range from 4 to almost 7 and do not show a systematic dependence on H_2O content. Extrapolating the equation of state of anhydrous Mg-wadsleyite to 20 GPa by using K_0' of 5 instead of 4 would result a 0.5% difference in density, which is significant in seismic observations. Moreover, K_0 and K_0' derived from least squares fitting *P-V* data sets have intrinsic dependence between fitted variables, i.e., anticorrelation between K_0 and K_0' [*Bass et al*., 1981; *Bell et al*., 1987; *Bina*, 1995]. This anticorrelation, often ignored when comparing results across experiments, must be considered carefully when analyzing the effects of chemical composition on elastic properties.

In this study, we focus on accurately determining the effect of hydration on the difference in K_0' between nearly anhydrous and hydrous Fe-bearing wadsleyite. By simultaneously loading wadsleyite crystals of similar Fe content but significantly different H_2O contents into one diamond anvil cell experiment, we measured their relative volumes at each pressure and a direct comparison of K_0' is made without introducing bias from the pressure scales. Furthermore, the data sets are equivalent in that every volume measurement for each composition shares a common pressure point. In the comparative compressibility experiments, three Fe-bearing ($X_{Fe} = 0.10$) hydrous wadsleyite crystals containing 2.0 wt % H_2O were loaded together with three crystals having the same Fe content but only 0.25 wt % H_2O, an order of magnitude less water. In addition, we included a crystal of hydrous ringwoodite that was synthesized coexisting with the hydrous wadsleyite in order to constrain

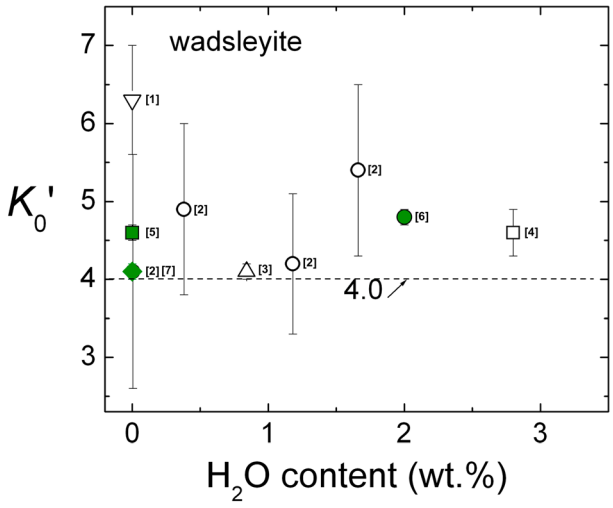

Figure 1. Pressure derivative of the bulk modulus, $K_0' = (dK/dP)_{P=0}$, versus H_2O content for Mg-wadsleyite (open symbols) and Fe-bearing wadsleyite (filled symbols) compiled from the experimental literature. References are [1] *Hazen et al.* [2000a], [2] *Holl et al.* [2008], [3] *Mao et al.* [2008], [4] *Yusa and Inoue* [1997], [5] *Li and Liebermann* [2000], [6] *Mao et al.* [2011], and [7] *Wang et al.* [2014].

the difference in K_0' between hydrous ringwoodite and hydrous wadsleyite. A highly focused synchrotron X-ray beam of ~10 μm diameter allowed the collection of individual diffraction patterns from the seven different crystals within the same diamond anvil cell. In addition, two internal pressure standards (MgO and ruby fluorescence) were employed and small pressure steps of <1 GPa up to 32 GPa facilitated fitting and analysis of a third-order Birch-Murnaghan equation of state to the pressure-volume data. The results constrain the relative value of K_0' between dry and hydrous wadsleyite and also between the coexisting hydrous Fe-bearing wadsleyite and ringwoodite. These results are used to evaluate the effect of iron and hydrogen on the bulk modulus of wadsleyite and ringwoodite at pressures relevant to the mantle transition zone.

2. Experimental Methods

2.1. Sample Synthesis

Single crystals of Fe-bearing hydrous wadsleyite and ringwoodite were synthesized in the 5000 t, multianvil press at Bayerisches Geoinstitut (run Z0570). Crystals of hydrous wadsleyite used in the high-pressure Brillouin spectroscopy study of *Mao et al.* [2011] came from the same synthesis run. Starting materials consisted of San Carlos olivine plus ~10 wt % H_2O added as liquid and welded into a Pt capsule 3 mm in height and diameter. The starting material was compressed to 18 GPa and heated to 1400°C. Heating duration was 1 min at 1400°C and then decreased to 1100°C and held for 20 min before quenching. The anhydrous wadsleyite (run Z0902) was synthesized from San Carlos olivine at 11 GPa and 1100°C using the same technique as run Z0570, but without the addition of H_2O.

2.2. Raman and FTIR Spectroscopy

Wadsleyite crystals from runs Z0570 and Z0920 were initially characterized by Raman spectroscopy. Unpolarized Raman spectra were obtained using a solid-state excitation laser with $\lambda_0 = 458$ nm and recorded from 120 to 4000 cm^{-1}. In the low-wave-number region, the hydrous (Z0570) and nominally anhydrous (Z0920) wadsleyite exhibit similar Raman spectra, both in the number and frequency of major vibrational modes (Figure 2a). At high wave number (Figure 2b), the O-H stretching modes are observed in both samples, indicating that some H_2O is incorporated into the nominally anhydrous sample Z0920 even though no water was intentionally added to the experiment. Although one cannot quantify the differences in intensity of the O-H stretching modes from unpolarized Raman spectra, the data shown in Figure 2b were collected with identical parameters. The intensity of the main O-H stretching band at 3358 cm^{-1} for the hydrous sample Z0570 is roughly 3 times higher than for the nominally anhydrous sample Z0920. The band is also shifted to lower wave numbers by about 30 cm^{-1} for the less hydrous sample, Z0920. A similar difference of intensity is observed in the second strongest O-H stretching band at 3576 cm^{-1}, but there is no difference in shift between the two samples (Figure 2b). Sample Z0570 displays a weak band at 3649 cm^{-1}, which is not observed in sample Z0902.

In order to further evaluate the difference in H_2O content between wadsleyite samples Z0570 and Z0920, unpolarized Fourier transform infrared (FTIR) spectra were obtained on three different randomly oriented crystals from each run (Figure 2c). Crystals were double polished with a final thickness of 18 ± 2 μm for all

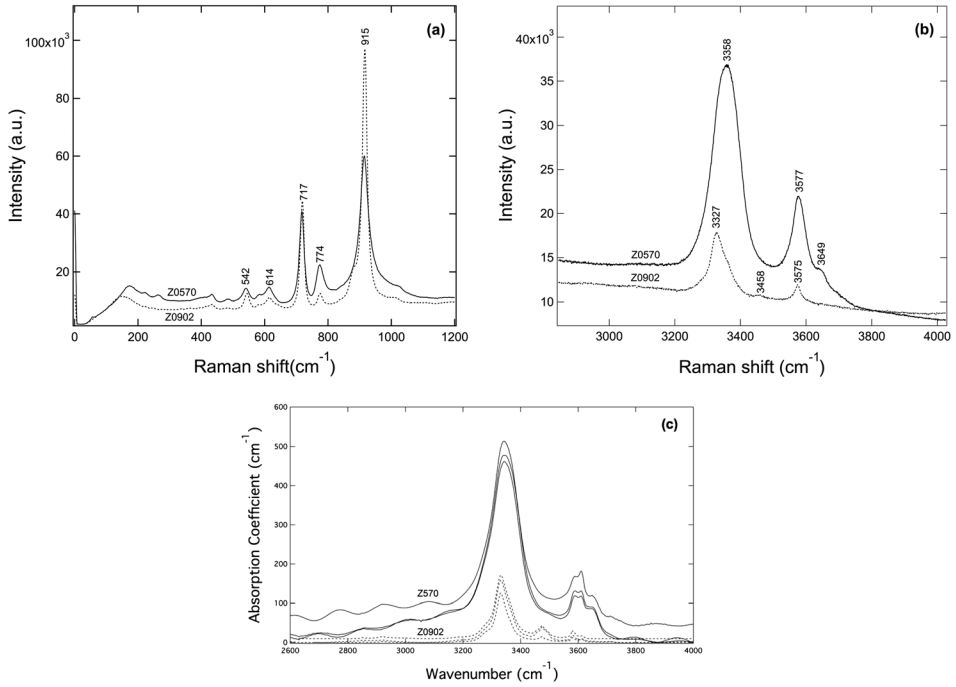

Figure 2. Unpolarized Raman and FTIR spectra of Fe-bearing wadsleyite Z0902 (dashed lines, 0.25 wt % H_2O) and Z0570 (solid lines, 2.0 wt % H_2O). (a) Raman spectra in the lattice mode region. (b) Raman spectra in the O-H stretching region. (c) Unpolarized FTIR spectra from three different crystals (random orientation) of each composition. All three crystals of Z0570 were 18 ± 2 μm thick (solid lines), giving a maximum absorbance of ~0.9. The crystals of Z0920 were 21 ± 2, 21 ± 2, and 46 ± 2 μm thick, going from the top to bottom spectrum (dashed lines).

samples from Z570, and for samples from Z0902 the three crystals were 21 ± 2, 21 ± 2, and 46 ± 2 μm thick. The maximum absorbance (for Z570) was 0.9. IR spectra were collected from 1850 to 4000 cm^{-1} with a globar light source, Bruker IFS 66v FTIR spectrometer, Hyperion microscope, and InSb detector. Following baseline correction, integrated absorbance and area-weighted averages of the peak positions were used to estimate the H_2O content of each sample using the wadsleyite-specific calibration of *Deon et al*. [2010]. By this method, we obtain 1.4 wt % H_2O for sample Z0570 and 0.25 wt % H_2O for sample Z0920.

2.3. Secondary-Ion Mass Spectrometry

The H_2O content of wadsleyite and ringwoodite from run Z0570 was also measured by secondary-ion mass spectrometry (SIMS). We present an interlaboratory comparison made by measuring the H_2O content of wadsleyite Z0570 crystals on two different instruments: first on the Cameca IMS-3F ion mass microanalyzer at Hokkaido University and subsequently on the Cameca NanoSIMS 50L at the Carnegie Institution of Washington, Department of Terrestrial Magnetism (DTM). Table 1 gives experimental parameters and results of the interlaboratory SIMS measurements. Briefly, on the IMS-3F instrument at Hokkaido University, five different crystals measuring 200 μm across or smaller were measured with at least two points per crystal. In the Hokkaido measurements, a natural amphibole crystal containing 1.66 wt % H_2O was used as a calibration standard, as described by *Miyagi et al*. [1998]. At Carnegie Institution on the NanoSIMS, three different silicate glasses containing 0.17, 1.00, and 1.62 wt % H_2O were used to develop a calibration against the measured mass ratios of $^{17}OH/^{28}Si$ [*Hauri et al*., 2006; *Saal et al*., 2008]. Further experimental details are provided in Table 1. The average H_2O content measured from 5 different crystals and 19 different measurement points at Hokkaido is 2.07(± 0.24) wt % H_2O. The Hokkaido SIMS measurements are in agreement within mutual experimental uncertainty with NanoSIMS results from DTM-Carnegie, where the average of 14 measurements points across one crystal was 1.93(± 0.22) wt % H_2O. We take the average of the interlaboratory results, 2.0(2) wt % H_2O, to be the best estimate of the water content of hydrous wadsleyite Z0570. The SIMS H_2O content of wadsleyite Z0570 is about 1.4 times (roughly 2–3σ) higher than suggested by FTIR using the *Deon et al*. [2010]

Table 1. Interlaboratory Comparison of Secondary-Ion Mass Spectrometry (SIMS) Parameters and Results for the H_2O Content Wadsleyite, Sample Z0570

Parameter	Experiment 1	Experiment 2
Facility	Hokkaido University	Carnegie DTM
Instrument	Cameca IMS-3F	Cameca NanoSIMS 50L
Beam	$^{16}O^-$	Cs^+
Voltage/current	12.5 kV/10 nA	8 kV/1 nA
Beam or raster size	30 μm diameter (beam)	$7 \times 7\ \mu m^2$ (raster)
Ion collection area	$10 \times 10\ \mu m^2$	$2.6 \times 2.6\ \mu m^2$
Measured ratio	$^1H^+/^{30}Si^+$	$^{17}OH/^{28}Si$
Standards	Amphibole (1.66 wt % H_2O)	Silicate glasses
		519-4 (0.17 wt % H_2O)
		D52-5 (1.00 wt % H_2O)
		D30-1 (1.62 wt % H_2O)
Detection limit sample	San Carlos olivine	Synthetic forsterite
Measured value	0.0049 wt % H_2O	0.0025 wt % H_2O
H_2O content (wt % H_2O)	Crystal 1	Crystal 6
	2.11	1.74
	1.90	1.75
	1.78	1.86
	2.65	1.88
	1.81	1.88
	2.41	2.04
	Crystal 2	2.35
	2.07	2.32
	1.97	1.64
	1.85	1.56
	Crystal 3	2.01
	2.31	2.04
	1.83	1.90
	Crystal 4	1.99
	2.15	
	2.03	
	2.30	
	2.22	
	Crystal 5	
	1.96	
	1.83	
	1.87	
	2.27	
Average wt % H_2O	2.07(24) wt % H_2O	1.93(22) wt % H_2O

calibration. Given the importance of hydrous wadsleyite to modeling the mineralogy and geochemistry of Earth's transition zone, future work on calibrating both spectroscopic and SIMS H_2O contents for wadsleyite against absolute methods is warranted [e.g., *Thomas et al*., 2015].

For the hydrous ringwoodite synthesized in run Z0570 and coexisting with hydrous wadsleyite, NanoSIMS measurements at DTM-Carnegie give an average from nine measurements across one crystal of 1.38 (± 0.30) wt % H_2O. The ratio of H_2O in wadsleyite to coexisting ringwoodite in experiment Z0570 is thus ~1.5, which is comparable to the hydrogen partitioning value of ~2 between wadsleyite and ringwoodite reported by *Inoue et al*. [2010]; in both cases wadsleyite contains more H_2O than the coexisting ringwoodite.

2.4. Major Element Chemistry: EMPA and Mössbauer Spectroscopy

The major element composition of wadsleyite and ringwoodite samples was determined by electron microprobe analysis (EMPA). The resulting $Mg/(Mg + Fe^{2+} + Fe^{3+})$ ratios were 0.90 and 0.89 for wadsleyite samples in run Z0902 and run Z0570, respectively. Samples from run Z0902 and run Z0570 both contain one Si per formula unit. The oxidation state of Fe in hydrous wadsleyite (run Z0570) was characterized by Mössbauer spectroscopy. A piece of 25 μm thick Ta foil (absorbing 99% of 14.4 keV gamma rays) drilled with either a 300 μm hole (sample 1) or 400 μm hole (sample 2) was centered over each crystal. The average thickness of the

crystals was estimated to be roughly 200 μm (sample 1) and 250 μm (sample 2), respectively, which combined with the composition of Fo_{90} (i.e., $X_{Fe} = 0.10$) implies an effective Mössbauer thickness of 6.9 and 8.6 mg Fe/cm^2 for samples 1 and 2, respectively. The Mössbauer spectra were recorded at room temperature (293 K) in transmission mode on a constant acceleration Mössbauer spectrometer with a nominal 370 MBq ^{57}Co high specific activity source in a 12 μm thick Rh matrix. The velocity scale was calibrated relative to a 25 μm thick α-Fe foil using the positions certified for (former) National Bureau of Standards standard reference material no. 1541; line widths of 0.36 mm/s for the outer lines of α-Fe were obtained at room temperature. The spectra were collected over 2 days (sample 1) and 1 day (sample 2), respectively, and were fitted using the commercially available fitting program NORMOS written by R.A. Brand (distributed by Wissenschaftliche Elektronik GmbH, Germany).

The Mössbauer spectra of hydrous Fe-bearing wadsleyite from run Z0570 are dominated by an asymmetric quadrupole doublet with less intense absorption between the main components (Figure 3). The dominant absorption was fitted to a single Fe^{2+} doublet, and the remaining absorption was modeled using a doublet corresponding to Fe^{3+}. Conventional constraints were applied to the components of each Fe^{3+} doublet (i.e., equal widths and areas), while only the widths of the Fe^{2+} components were constrained to be equal. The area ratios of the Fe^{2+} doublet components were allowed to vary, due to the effects of preferred orientation arising from the single-crystal nature of the sample. In addition, the center shift of the Fe^{3+} doublet from sample 1 was constrained to the value obtained from the spectrum for sample 2. All spectral components were assumed to have Lorentzian line shape. Estimated standard deviations were derived from the statistics of the fitting process as well as uncertainties in the fitting model itself. The hyperfine parameters derived from the fits are listed in Table 2.

The center shifts and quadrupole splitting values for the Fe^{2+} and Fe^{3+} doublets are consistent within experimental uncertainty with values previously observed for hydrous wadsleyite [*Bolfan-Casanova et al*., 2012]. The values of $Fe^{3+}/\Sigma Fe$ were calculated from the relative areas of the Fe^{3+} absorption. The resulting average of $Fe^{3+}/\Sigma Fe$ in sample Z0570 is about 10%. Although the ratio $Fe^{3+}/\Sigma Fe$ of the sample in run Z0902 was not characterized, it is expected to be very low because of the low water content in this sample [*McCammon et al*., 2004]. After the chemical compositions were known, the chemical formulae of the samples in run Z0902 and run Z0570 were determined to be $(Mg^{2+}_{1.782}Fe^{2+}_{0.198})H_{0.041}SiO_4$ and $(Mg^{2+}_{1.638}\ Fe^{2+}_{0.173}Fe^{3+}_{0.019})H_{0.320}SiO_4$ based on charge balance, water content, $Mg/(Mg + Fe^{2+} + Fe^{3+})$ ratio, and $Fe^{3+}/\Sigma Fe$ ratio. The same chemical analyses were applied to the Fe-bearing ringwoodite (Z0570) sample used in this experiment, yielding the chemical formula $(Mg^{2+}_{1.577}\ Fe^{2+}_{0.291}Fe^{3+}_{0.032})H_{0.227}Si_{0.985}O_4$.

2.5. High-Pressure Single-Crystal X-Ray Diffraction

Before carrying out the high-pressure experiment, initial lattice parameters of samples under ambient conditions were measured using a four-circle X-ray diffractometer at the University of Colorado Boulder. Single-crystal lattice parameters were refined using the program SINGLE [*Angel and Finger*, 2011]. The low-H_2O wadsleyite sample (run Z0902) is orthorhombic, whereas hydrous wadsleyite (Z0570) is slightly monoclinic with $\beta = 90.078(2)°$. Room pressure lattice parameters of the hydrous wadsleyite were also refined with orthorhombic symmetry for comparison with subsequent high-pressure X-ray diffraction (XRD) data collected at the synchrotron. Lattice parameters, density, and molar volume of the samples used in this study are reported in Table 3.

High-pressure, single-crystal X-ray diffraction was carried out at beamline 16-ID-B, HPCAT, Advance Photon Source, Argonne National Laboratory. The wavelength of the monochromatic synchrotron radiation X-ray was $\lambda = 0.407376$ Å, calibrated using a CeO_2 standard. Diffraction images were recorded by a MAR CCD detector, positioned 21.32 cm from the sample. A symmetric-piston diamond cell, fitted with diamond anvils having 300 μm culets, was used. A rhenium gasket was preindented to about 30 μm initial thickness, and a hole approximately 200 μm in diameter was eroded using an electrostatic discharge machine. The diamond anvil cell was also fitted with one cubic boron nitride seat, placed downstream of the synchrotron X-ray source to allow wide-angle access to diffracted X-rays, while a slit tungsten carbide seat was used in the upstream side. This setup allowed oscillation of the cell about the vertical axis by ±14°. Three single-crystal anhydrous wadsleyites (run Z0902) as well as three single-crystal hydrous wadsleyites (run Z0570) and one crystal of hydrous ringwoodite (run Z0570) were loaded together into the same diamond anvil cell, as shown in Figure 4.

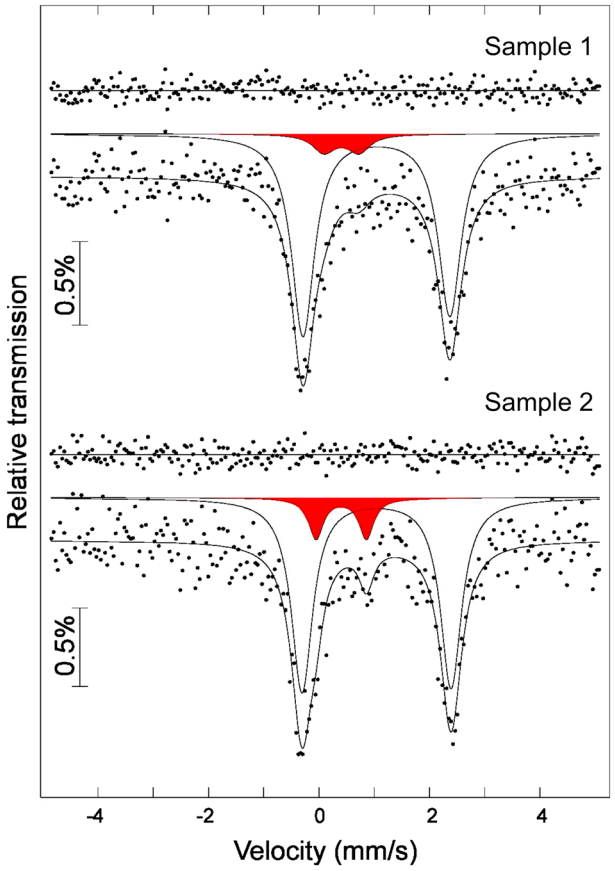

Figure 3. Mössbauer spectra of two different hydrous wadsleyite crystals (labeled sample 1 and sample 2) from run Z0570. The absorption assigned to Fe^{3+} is indicated in red and constitutes an average of about 10% of the total Fe in the sample.

By loading three crystals, each of hydrous and anhydrous wadsleyite together in the same diamond anvil cell, we achieved better *hkl* coverage. The cell was loaded with neon as pressure medium using the COMPRES/GSECARS gas loading system at Advanced Photon Source [*Rivers et al*., 2008]. Two pressure standards were also included in the cell; a single-crystal of MgO and an annealed ruby sphere, for the purpose of comparing the results from two pressure scales on the fitted K_0'. The pressure inside the cell was about 1.09 GPa after gas loading, and the gasket hole shrank to 75% of its original size. Neon was chosen in this experiment for its ability to retain a quasi-hydrostatic state up to 80 GPa [*Dewaele et al*., 2008], which enables it to maintain similar pressure environments surrounding every crystal inside the cell.

Because K_0' is the second derivative of a *P-V* curve, a precise determination of pressures and fine pressure steps are critical in constraining K_0' in a high-pressure compression experiment. In order to better constrain the equation of state, a gas membrane cell as well as an online ruby system was set up to control small pressure increments of 0.5–0.8 GPa per step up to 32 GPa. After increasing pressure at each pressure step, the cell was allowed to settle for 10–15 min before performing XRD to ensure that pressure was stable during measurements. Three annealed ruby spheres were loaded along with samples into the pressure chamber as pressure markers. The ruby sphere at the center of the cell served as the primary marker, while the other two at the edges were used for checking pressure gradients. The ruby pressure was calibrated from the measured shift (λ/λ_0) of the *R*1 ruby fluorescence line using P (GPa) $= A/B\{[1 + (\Delta\lambda/\lambda_0)]^B - 1\}$, where $A = 1904$ and $B = 10.32$ [*Jacobsen et al*., 2008]. The reported ruby pressure in this paper is the average of pressures measured before and after collecting XRD images, which did not differ by more than 0.2 GPa. A single-crystal of MgO was also loaded into the pressure chamber as a secondary pressure marker. MgO pressures were calculated using the third-order Birch-Murnaghan (BM) equation of state (EOS) with initial volume $V_0 = 74.698$ (Å^3), $K_{T0} = 160.32$ GPa, and $K_0' = 4.08$ [*Kennett and Jackson*, 2009]. Uncertainties of MgO pressures were estimated following the procedures described in *Angel et al*. [1997].

Table 2. Results From Mössbauer Spectroscopy[a], Wadsleyite Sample Z0570

	CS (mm/s) (Relative to α-Fe)	QS (mm/s)	FWHM (mm/s)	Area
		Crystal 1		
Fe^{2+}	1.04(1)	2.66(5)	0.50(5)	0.92(5)
Fe^{3+}	0.4[b]	0.63(16)	0.49(27)	0.08(5)
		Crystal 2		
Fe^{2+}	1.04(1)	2.70(5)	0.46(5)	0.87(6)
Fe^{3+}	0.40(5)	0.91(10)	0.32(12)	0.13(6)

[a]CS = center shift ; QS = quadrupole Splitting; FWHM = full width at half maximum.
[b]Constrained to the value obtained from crystal 2.

Table 3. Composition, Lattice, and Density Parameters of Samples Used in This Study

Run #	Z0902-β Phase	Z0570-β Phase	Z0570-γ Phase
$Mg/\Sigma(Mg + Fe^{2+} + Fe^{3+})$	0.90	0.89	0.83
$Fe^{3+}/\Sigma Fe$ (%)	very low	~10%	~10%
H_2O content (wt %)	~0.25	2.0	1.38
Lattice parameters	$\beta_0 = 90°$ $a_0 = 5.7045(4)$ Å $b_0 = 11.4765(4)$ Å $c_0 = 8.2707(4)$ Å $V_0 = 541.46(5)$ Å^3	$\beta_0 = 90°$ $a_0 = 5.6918(10)$ Å $b_0 = 11.5276(10)$ Å $c_0 = 8.2641(8)$ Å $V_0 = 542.23(12)$ Å^3 $\beta_0 = 90.078(2)°$ $a_0 = 5.6929(2)$ Å $b_0 = 11.5275(2)$ Å $c_0 = 8.2648(1)$ Å $V_0 = 542.37(2)$ Å^3	$a_0 = 8.1011(4)$ Å $V_0 = 531.65(8)$ Å^3
Atomic mass, M (g/mol)	146.48	143.45	147.82
Density, ρ_0 (g/cm^3)	3.595	3.515	3.695
Molar volume, MV (mol/cm^3)	40.75	40.81	40.00

To obtain the orientation matrix at the initial pressure of 1.09 GPa, an ω step scan was performed on each crystal in the range from −14 to 14°, with step size 1°, and exposure time 2 s per image. These resulting 29 images were used to calculate the unit cell parameters and determine the peak positions. The peak positions for all crystals were assigned using the software GSE_ADA [*Dera*, 2007a, 2007b]. A wide ω scan was performed thereafter at subsequent pressure steps in the range from −14 to 14° with exposure time 28 s on each crystal. For each composition, the unit cell parameters were refined by combining peaks collected from all three crystals in unit cell [*Holland and Redfern*, 1997]. The number of available peaks decreased with increasing pressure. In order to maintain consistency, only the peaks appearing in all pressure steps were included for high-pressure lattice parameter refinement. Thus, 52 diffracted peaks for sample Z0902 and 69 diffracted peaks for sample Z0570 were included in the unit cell analyses. Although there were only six diffracted peaks available for the hydrous ringwoodite sample, they were sufficient for the purpose of determining the cubic lattice parameters.

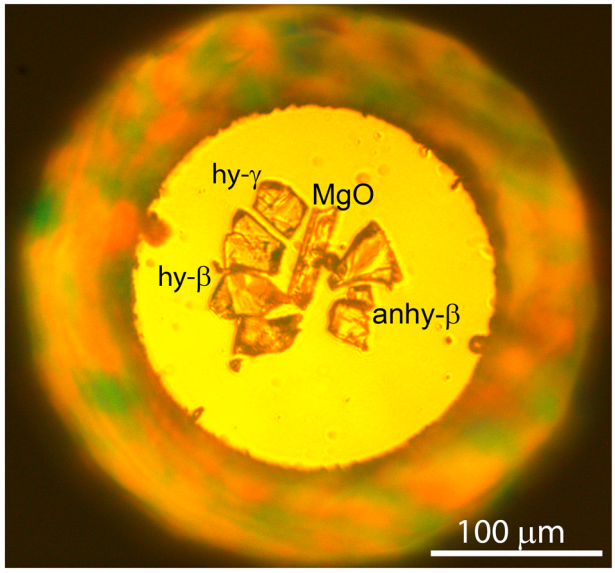

Figure 4. Diamond anvil cell setup for the comparative compressibility study, at room pressure before loading with neon. There are three single crystals of wadsleyite from run Z0902 (labeled anhy-β), three single crystals of wadsleyite from run Z0570 (labeled hy-β), and a crystal of coexisting ringwoodite from run Z0570 (labeled hy-γ). A single-crystal MgO and three ruby spheres were also included for pressure calibration.

3. Results and Discussion

3.1. Influence of Fe and H_2O on Lattice Parameters and Density of Wadsleyite

Whereas Fe increases all three lattice parameters of wadsleyite, H_2O decreases a and c but increases the b axis, as illustrated in Figure 5. The Fe-bearing wadsleyite sample Z0902 (0.25 wt % H_2O) lattice parameters are $a_0 = 5.7045(4)$, $b_0 = 11.2707(4)$, and $c_0 = 8.2707(4)$ Å, compared with the very hydrous (2.0 wt % H_2O) and slightly monoclinic sample Z0570 with $a_0 = 5.6929(2)$, $b_0 = 11.5275(2)$, $c_0 = 8.2648(1)$ Å, and $\beta = 90.078(2)°$. Refining the lattice parameters of sample Z0570 in the orthorhombic system gives $a_0 = 5.6918(10)$, $b_0 = 11.5276(10)$, and $c_0 = 8.2641(8)$ Å. The unit cell refinements in this study further confirm that hydration lowers the symmetry of wadsleyite from *Imma* to *I2/m* [*Smyth et al.*, 1997; *Holl et al.*, 2008; *Jacobsen et al.*, 2005;

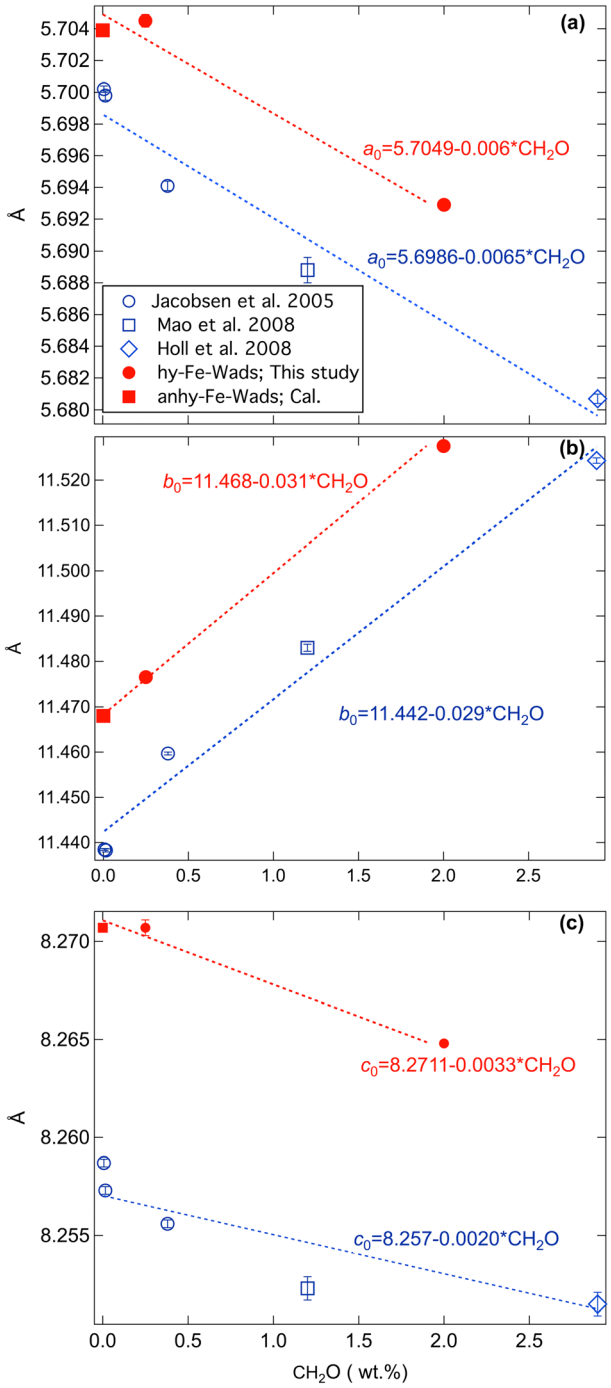

Figure 5. Variation of lattice parameters with H_2O content in Mg-wadsleyite (blue) and Fe-bearing wadsleyite (red). The dash lines represent linear regressions.

Kudoh et al., 1996]. Violation of orthorhombic symmetry can be attributed to the ordering of divalent cation vacancies onto nonequivalent M3 sites, breaking the mirror symmetry element perpendicular to the *b* axis [*Smyth et al.*, 1997].

To better constrain the combined effects of Fe and H_2O on wadsleyite lattice parameters, we first quantified the effects of Fe and H_2O separately, based on this and previous studies using data listed in Table 4 and plotted in Figure 5. *Finger et al.* [1993] investigated the effects of Fe on the structure of wadsleyite and showed that Fe prefers the M3 and M1 sites over the M2 site. The effect of iron on lattice parameters estimated from the anhydrous Fe-bearing wadsleyite data [*Finger et al.*, 1993] shows that increasing X_{Fe} by 0.10 increases a_0, b_0, and c_0 by 0.011, 0.017, and 0.016 Å, respectively. Analyzing the effects of hydration on Mg- and Fe-bearing wadsleyite requires a systematic approach to determining the water content.

In order to eliminate issues associated with comparing samples characterized by different methods (FTIR, Raman, or SIMS), we redetermined the water content of several Mg-wadsleyite samples from the same synthesis runs as previous FTIR and elasticity studies using NanoSIMS. We followed the same procedure described above for sample Z0570. In particular, we analyzed the water content of WS3056 and WH833 from the study of *Jacobsen et al.* [2005], sample WH2120 from *Mao et al.* [2008], and sample SS0401 from the study of *Holl et al.* [2008]. Referring to Table 4, the H_2O content of WS3056 was previously determined by the calibration of *Paterson* [1982]. The H_2O content of WH833 was previously determined by the calibration of *Libowitzky and Rossman* [1997]. The H_2O contents of WH2120 and SS0401 were previously determined by the *b*/*a* axial ratio calibration of *Jacobsen et al.* [2005], which was tied largely to *Paterson* [1982]. The FTIR water contents of the current samples, Z0570 and Z0920, are reported from the mineral-specific calibration of *Deon et al.* [2010]. For sample Z0570, the maximum absorbance was around 0.9 and we found for a mean wave number of 3380 cm^{-1}, the *Deon et al.* [2010] calibration leads to a 1.2 times higher water content than *Libowitzky and Rossman* [1997] and 1.6 times higher value than *Paterson* [1982]. The H_2O contents measured previously by FTIR and the new NanoSIMS results are listed in Table 4 and plotted in Figure 6.

Table 4. Compilation of Fe and H_2O Content by Different Methods and Lattice Parameters of Hydrous Wadsleyite

Sample	X_{Fe}	H_2O (wt %; FTIR)	H_2O (wt %; SIMS)	a (Å)	b (Å)	c (Å)	V (Å^3)	ρ_0 (kg/m^3)	Reference
WS3056	0	0.005[a]	0.006(3)[f]	5.7002(2)	11.4385(2)	8.2587(2)	538.46(2)	3472	*Jacobsen et al.* [2005]
WZ304	0	0.015[a]		5.6998(2)	11.4383(3)	8.2573(2)	538.34(3)	3473	*Jacobsen et al.* [2005]
WH833	0	0.37(1)[b]	0.38(8)[f]	5.6941(2)	11.4597(3)	8.2556(2)	538.70(3)	3455	*Jacobsen et al.* [2005]
WH2120	0	0.84(8)[c]	1.20(7)[f]	5.6888(6)	11.4830(8)	8.2523(6)	539.08(8)	3418	*Mao et al.* [2008]
SS0401	0	1.66(17)[c]	2.9(2)[f]	5.6807(3)	11.5243(6)	8.2515(6)	540.20(5)	3338	*Holl et al.* [2008]
Fe00	0	0[d]		5.6921(2)	11.460(1)	8.253(2)	538.3(2)	3472	*Finger et al.* [1993]
Fe08	0.08	0[d]		5.7037(9)	11.4681(8)	8.2679(9)	540.1(1)	3585	*Finger et al.* [1993]
Fe16	0.16	0[d]		5.7119(9)	11.4681(8)	8.2799(9)	542.4(1)	3693	*Finger et al.* [1993]
Fe25	0.25	0[d]		5.717(1)	11.506(1)	8.299(1)	545.9(2)	3807	*Finger et al.* [1993]
Fe40	0.40	0[d]		5.739(2)	11.515(2)	8.316(1)	549.6(2)	4010	*Finger et al.* [1993]
Z0902	0.10	0.25[e]		5.7045(4)	11.4765(4)	8.2707(4)	541.46(5)	3595	This study
Z0570	0.11	1.4[e]	2.0(2)[f]	5.6929(2)	11.5275(2)	8.2648(1)	542.37(2)	3515	This study

[a]Calibration of *Paterson* [1982].
[b]Calibration of *Libowitzky and Rossman* [1997].
[c]X-ray diffraction, *b*/*a* axial ratio method of *Jacobsen et al.* [2005].
[d]Not measured, assumed nominally anhydrous.
[e]Current study, calibration of *Deon et al.* [2010].
[f]Current study, NanoSIMS measurements.

The discrepancy between the H_2O content determined by various FTIR calibrations and by NanoSIMS appears negligible when the water content is lower than ~0.5 wt % (Figure 6). However, for higher H_2O content we observe a factor of about 1.5 difference between SIMS and FTIR, with SIMS giving systematically higher water contents, even when compared with the calibration of *Deon et al.* [2010] for sample Z0570. One reason why SIMS could show higher H_2O contents would be due to small inclusions of very hydrous phases, such as superhydrous phase B. However, FTIR measurements would reveal such inclusions, which have not been observed in any of the wadsleyite crystals. It is more likely that FTIR spectra from the previous studies underestimated the H_2O content, either because polarized measurements did not use a mineral-specific calibration, because unpolarized measurements did not sample enough directions to build a statistically significant sampling of total absorbance, or because in very hydrous samples the main O-H stretching band of wadsleyite completely absorbed the light.

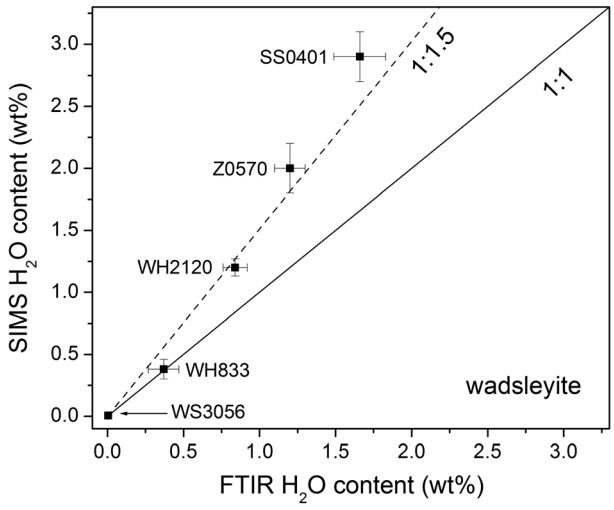

Figure 6. H_2O content of five wadsleyite samples measured by SIMS (this study), in comparison with water contents reported by FTIR in original studies: WS3056 from *Jacobsen et al.* [2005] and *Holl et al.* [2008] is nearly anhydrous with only 0.005–0.006 wt % H_2O as measured by both FTIR and SIMS (Table 4); WH833 from *Jacobsen et al.* [2005] and *Mao et al.* [2008] used the polarized-FTIR calibration of *Libowitzky and Rossman* [1997]; WH2120 and SS0401 from the study of *Mao et al.* [2008] from *b*/*a* axial ratio method [*Jacobsen et al.*, 2005], which is tied largely to FTIR calibrations of *Paterson*, [1982] and *Libowitzky and Rossman* [1997]; Z0570 from the current study gives 1.2 wt % H_2O using *Libowitzky and Rossman* [1997] or 1.4 wt % H_2O (as plotted) using the FTIR calibration of *Deon et al.* [2010]. The SIMS measurement of Z0570 was conducted on six different crystals, up to 14 points per crystal, using two different ion probes and calibration methods (see Table 2 for details).

Regression analyses of the effect of Fe and H_2O on the lattice parameters of wadsleyite are shown in Figure 5. Incorporation of 1 wt % H_2O in the Mg end-member wadsleyite causes the *a* and *c* axes of the wadsleyite to contract by ~0.001 and 0.005 Å, respectively, whereas the *b* axis expands by 0.036 Å. As seen in Table 4, uncertainty in the individual lattice parameters is typically in the fourth decimal place. The influence of 0.10 X_{Fe} on b_0 is only half that of incorporating 1 wt % H_2O into Mg-wadsleyite. In contrast, the influence of 0.10 X_{Fe} on a_0 and c_0 is more significant than adding 1 wt % H_2O (Figure 5).

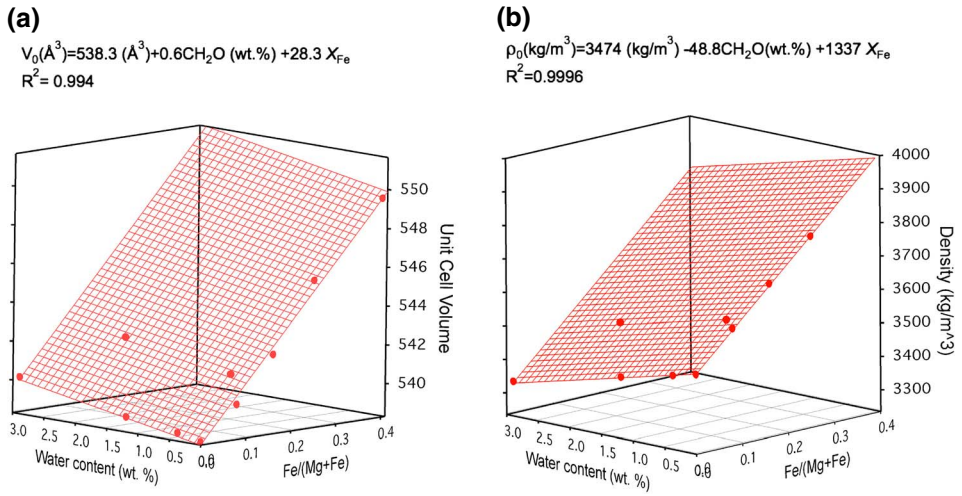

Figure 7. (a) The unit cell volume of Mg- and Fe-wadsleyite samples listed in Table 4 as a function of both Fe and H_2O content; (b) the variation of density (ρ_0) with Fe and H_2O content (in wt %). The blue meshes represent the planar regression fitting results.

To quantify the combined effects of Fe and H_2O, we carried out a 3-D planar multivariable linear regression analysis using all of the data listed in Table 4. The substitution of Mg by Fe and incorporation of H_2O into wadsleyite both expand the unit cell volume, as illustrated in Figure 7a. A 3-D fit to all of the data in Table 4 yields the following relationship for V_0 of wadsleyite:

$$V_0\left(\text{Å}^3\right) = 538.3(\pm0.6)\left(\text{Å}^3\right) + 0.6(\pm0.2)C_{H2O}(\text{wt }\%) + 28.3(\pm1.7)X_{Fe}, \quad (1)$$

with a regression fitting parameter of $R^2 = 0.9936$ and $\chi^2 = 0.848$. The variation of initial density (ρ_0) with Fe and H_2O content (in wt %) is illustrated in Figure 7b with fitted relationship:

$$\rho_0\left(\text{kg/m}^3\right) = 3474\ (\pm4)\ \left(\text{kg/m}^3\right) - 49(\pm3)C_{H2O}(\text{wt }\%) + 1337(\pm24)X_{Fe}, \quad (2)$$

with regression fitting parameter of $R^2 = 0.9996$ and $\chi^2 = 169.154$. Variation of the reference density of wadsleyite with both Fe and H_2O content will serve as an important anchor for high-pressure equations of state in this system.

3.2. Influence of Fe and H_2O on the *P-V* Equation of State of Wadsleyite

To investigate combined influence of Fe and H_2O on the *P-V* equation of state of wadsleyite, unit cell volumes of sample Z0902 and sample Z0570 at high pressures were collected and analyzed as described in section 2. The resulting pressure-volume data of wadsleyite Z0902, wadsleyite Z0570, ringwoodite Z0570, and MgO are listed in Table 5. As shown in Figure 8, the initial unit cell volume (V_0) of sample Z0570 (2.0 wt % H_2O) is about 0.14% larger than V_0 of Z0902 (with 0.25 wt % H_2O), but because the hydrous sample is more compressible, a volume crossover occurs at about 6 GPa. Although the hydrous sample has a smaller unit cell volume above 6 GPa, it remains less dense across the experimental pressure range (Figure 9) because of its lower atomic mass (Table 3). The density difference between hydrous (Z0570) and the nominally anhydrous (Z0902) wadsleyite is ~2.8%, a relationship which remains unchanged up to the maximum pressure of the experiment at 32 GPa, suggesting a very similar value of K_0'.

Pressure-volume data were fitted to a second- and third-order Birch-Murnaghan equation of state (BM-EOS) using EoSFIT7 [*Angel et al*., 2014]. In our procedure, V_0 and K_{T0} were refined for both second- and third-order BM equations. The value of K_0' was also refined for the third-order BM-EOS fitting, while K_0' has an implied value of 4 in the second-order BM-EOS fitting. The uncertainties in pressure and volume measurements were used as weights. Prior to fitting, we tested the reliability of ruby pressures in this experiment by fitting the *P-V* data of MgO (Table 5) to a third-order BM-EOS. The resulting equation of state is $V_0 = 74.69(2)$ Å^3, $K_{T0} = 163(2)$ GPa with $K_{T0}' = 4.05(21)$, in excellent agreement with previous static compression, ultrasonic, Brillouin, and theoretical studies [e.g., *Dorogokupets*, 2010; *Jaocbsen et al*., 2002; *Jacobsen et al*., 2008; *Kennett and Jackson*, 2009; *Mukherjee et al*., 2013; *Speziale et al*., 2001; *Tange et al*., 2009; *Wu et al*., 2008; *Zha et al*., 2000]. This result gives us confidence to use ruby pressures as the pressure marker in this study, although

Table 5. Volume-Pressure Data From Single-Crystal X-ray Diffraction of Samples Compressed in the Same Diamond Anvil Cell[a]

P_{ruby} (GPa)	Wadsleyite (Z0902)	Wadsleyite (Z0570)	Ringwoodite (Z0570)	MgO
1.0	538.76(3)	539.92(2)	528.73(5)	74.33(1)
1.7	536.32(3)	537.41(2)	526.14(6)	73.97(1)
2.3	534.43(3)	535.19(2)	524.75(7)	73.58(1)
3.0	532.57(2)	533.21(2)	522.65(5)	73.40(1)
3.4	531.32(3)	532.05(1)	522.20(5)	73.23(1)
4.0	529.43(3)	530.22(1)	519.54(6)	72.91(1)
4.4	527.99(3)	528.65(1)	519.24(5)	72.74(1)
5.7	524.47(2)	--	515.88(6)	72.20(1)
6.3	--	522.97(2)	514.13(5)	72.05(1)
7.1	--	--	512.83(6)	71.71(1)
8.2	517.30(3)	517.59(2)	509.14(6)	71.25(1)
9.0	515.58(2)	515.48(2)	506.58(5)	70.98(1)
10.3	512.97(2)	512.09(2)	504.46(6)	70.57(1)
11.1	511.29(2)	510.01(2)	502.48(5)	70.39(1)
12.1	508.62(2)	507.41(2)	500.51(6)	69.99(1)
13.1	506.37(2)	505.36(2)	497.83(5)	69.67(1)
14.1	504.15(2)	502.18(2)	496.10(7)	69.27(1)
15.1	501.95(2)	499.55(2)	493.91(5)	68.93(1)
16.2	498.97(3)	496.80(2)	491.57(5)	68.72(1)
17.2	496.78(3)	495.45(2)	487.44(6)	68.27(1)
18.4	494.20(2)	492.60(2)	486.57(5)	67.93(1)
19.6	492.01(2)	490.09(2)	484.04(5)	67.79(1)
20.8	489.11(2)	487.85(2)	482.24(5)	67.56(1)
22.2	485.85(2)	485.61(2)	478.79(5)	66.94(1)
23.3	484.35(2)	482.40(2)	477.44(6)	66.55(1)
24.3	482.00(2)	480.13(2)	475.67(5)	66.44(1)
25.5	480.69(2)	477.66(2)	473.08(4)	66.15(1)
26.3	478.72(2)	476.10(2)	471.46(4)	65.81(1)
27.5	476.71(2)	473.87(2)	469.30(4)	65.76(1)
28.3	475.57(2)	472.46(2)	468.42(4)	--
29.6	472.50(2)	469.99(2)	465.75(4)	65.04(1)
30.8	471.69(2)	468.06(2)	464.21(4)	64.78(1)
31.9	468.56(2)	466.19(2)	462.34(4)	64.51(1)

[a]Unit cell volumes are in Å^3. Uncertainty in the ruby pressure is ±0.1 GPa based on *P* measured before and after measurement of sample volume.

we stress, because the volume of each sample was measured at the same pressure in a single experiment, we ultimately aim to determine if there is any difference in the fitted K_0' of hydrous versus anhydrous wadsleyite, independent of the secondary pressure scale.

The resulting second-order BM-EOS parameters are $V_0 = 542.0(2)$ Å^3, $K_{T0} = 166(1)$ GPa and $V_0 = 543.4(2)$ Å^3, $K_{T0} = 153(1)$ GPa for slightly hydrous (Z0902) and very hydrous (Z0570) wadsleyite, respectively. The same pressure-volume data were fitted to the third-order BM-EOS, resulting in $V_0 = 541.6(2)$ Å^3, $K_{T0} = 170(2)$ GPa, and $K_{T0}' = 3.72(16)$ for slightly hydrous (Z0902) and $V_0 = 543.1(3)$ Å^3, $K_{T0} = 157(2)$ GPa, and $K_{T0}' = 3.77(14)$ for the very hydrous (Z0570) wadsleyite. The second-order BM-EOS obtained for hydrous ringwoodite (run Z0570) gives $V_0 = 532.0(2)$ Å^3 and $K_{T0} = 172(1)$, with parameters $V_0 = 531.6(3)$ Å^3, $K_{T0} = 177(3)$ GPa, and $K_{T0}' = 3.7(2)$ for the third-order BM-EOS. All values of K_{T0}' resulting from this experiment are lower than the reported values of K_0' from previous studies, which range from 4.0 to 7.1 (Figure 1).

Two approaches were taken to test our fitting results. First, the same data sets were fitted to second- and third-order BM equations of state using the MgO pressure marker, resulting in EOS parameters that are identical within error to the results using ruby pressures. In order to determine whether the improvement in fit to the data achieved by using a third-order BM-EOS (in which the value of K_{T0}' is a free parameter) rather than second-order BM (in which K_{T0}' is by definition fixed at a value of 4) is statistically meaningful, we performed *F* test analyses for the addition of the free parameter [*Bevington*, 1969]. The results show that the deviation of K_{T0}' from the reference value of 4 is statistically significant at the 96% confidence level for sample Z0902 and

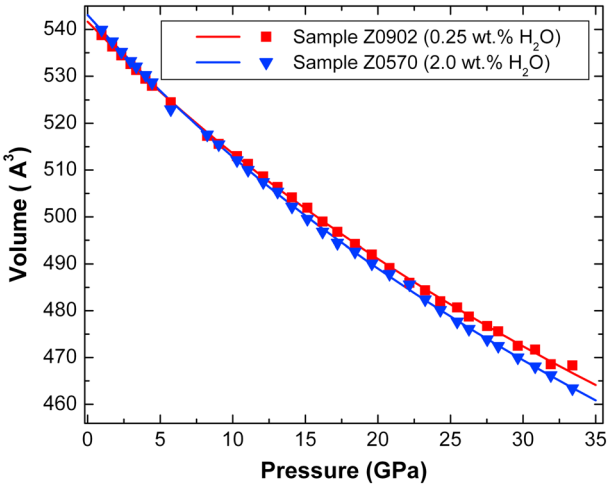

Figure 8. Volume-pressure data for anhydrous (red, Z0902) and hydrous (blue, Z0570) Fe-bearing wadsleyite and fitted equations of state (solid curves) given in the text. Although hydrous wadsleyite has a larger cell volume at room pressure, a crossover occurs at about 6 GPa due to the higher compressibility of the hydrous sample.

the 94% confidence level for both beta and gamma phases of Z0570. The low K_{T0}' values of Fe-bearing wadsleyite observed in this study are likely caused by the combined influences of Fe and H_2O in wadsleyite, rather than by experimental issues, as the resulting K_{T0}' of MgO within the same pressure chamber is 4.05(21), which is consistent with previous studies, e.g., 4.08(4) from the simultaneous nonlinear inversion of multiple data sets performed by *Kennett and Jackson* [2009].

To better visualize the quality of EOS fits, a plot of normalized stress $F_E = P/3f_E(1+2f_E)^{5/2}$ versus Eulerian strain $f_E = [(V_0/V)^{2/3} - 1]/2$ (an F_E-f_E plot) was constructed as shown in Figure 10. The unusual curvature of the F_E-f_E plot at very low strain for wadsleyite Z0570 calculated using the measured V_0 (shown in the inset in Figure 10) indicates that the V_0 measured by the four-circle X-ray diffractometer is not compatible with the high-pressure volumes collected using the synchrotron X-ray diffractometer. We therefore excluded the measured four-circle V_0 from our *P-V* data and carried out the final least squares fitting following the method described in previous paragraphs. Because V_0 is a prerequisite for calculating the Eulerian finite strain, the measured V_0 was replaced with V_0 obtained from the third-order BM equation of state to calculate the experimental Eulerian finite strain in the F_E-f_E plot reported here. As seen in Figure 10, the EOS of both Z0902 and Z0570 are well constrained by the data and have slightly negative slopes in this F_E-f_E plot, indicating that the values of K_{T0}' are smaller than 4.0. The regression lines for Z0902 and Z0570 data points are almost parallel to each other. Our results suggest that increasing H_2O from 0.25 to 2.0 wt % H_2O in Fe-bearing wadsleyite reduces the isothermal bulk modulus (K_{T0}) from 170 (2) GPa to 157(2) GPa, a reduction of 10.5%, but hydration does not affect the pressure derivative.

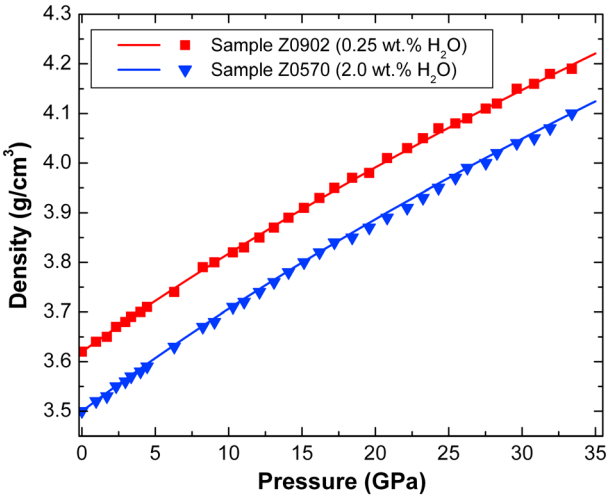

Figure 9. Variation of density with pressure for anhydrous (red, Z0902) and hydrous (blue, Z0570) Fe-bearing wadsleyite from the current compression experiments.

Before discussing the combined influence of Fe and H_2O on the compressibility of wadsleyite, we briefly review the independent effects of Fe and H_2O on the compressibility of wadsleyite separately. Many studies have examined the effect of Fe on elastic properties of wadsleyite [e.g., *Hazen et al.*, 2000a; *Hazen et al.*, 2000b; *Li and Gwanmesia*, 1996; *Li and Liebermann*, 2000; *Liu et al.*, 2009; *Wang et al.*, 2014; *Zha et al.*, 1997]. Experimental results suggest that Fe has an insignificant effect on the bulk modulus ($K_{T,S0}$) of anhydrous wadsleyite: the bulk modulus of 0.0 X_{Fe} wadsleyite is ~170(2) GPa [*Li and Gwanmesia*, 1996; *Zha et al.*, 1997; *Hazen et al.*, 2000a], 0.075 X_{Fe} wadsleyite is 170(3) GPa [*Wang et al.*, 2014], 0.12 X_{Fe} wadsleyite is ~172(2) GPa [*Li and Liebermann*, 2000],

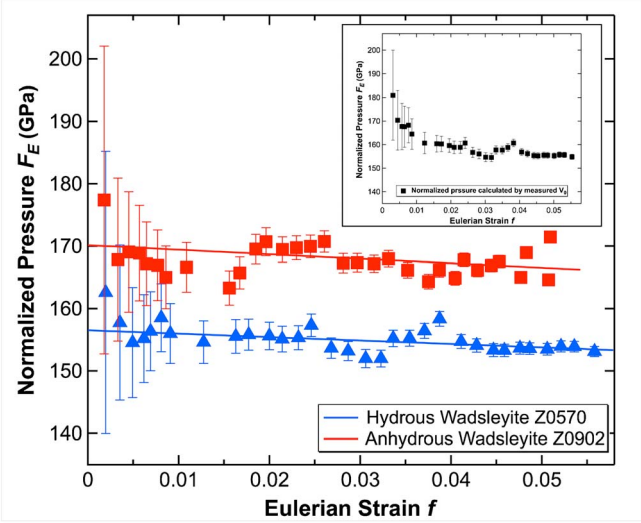

Figure 10. Plot of the normalized (Birch) pressure (F_E) versus Eulerian strain (f) for anhydrous (red) and hydrous (blue) wadsleyite. Data were calculated using the fitted V_0 obtained from the third-order BM equations of state. The inset shows the F_E of sample Z0570 calculated using the measured V_0 at ambient conditions. The curvature toward high F_E at very low strain indicates the measured V_0 from a separate experiment is not compatible with the high-pressure data and therefore not used in the final equation of state fitting.

and 0.25 X_{Fe} wadsleyite is ~173(3) GPa [*Hazen et al.*, 2000a]. Thus, upon increasing X_{Fe} from 0 to 25% the reported bulk modulus is invariant within experimental uncertainties. In contrast, H_2O has a much larger influence on the bulk modulus of wadsleyite. For hydrated Mg-wadsleyite, partially vacant octahedral sites (M3) associated with the incorporation of H_2O have a larger M3 site volume [*Jacobsen et al.*, 2005] resulting in a more compressible structure. This mechanism is reflected in the systematic reduction of bulk modulus $K_{T,S0}$ with increasing H_2O content [*Holl et al.*, 2008; *Mao et al.*, 2008; *Ye et al.*, 2010]. *Ye et al.* [2010] summarized Mg end-member wadsleyite experimental data and estimated that the incorporation of 1 wt % H_2O in wadsleyite causes a ~7% reduction in K_{T0}. *Mao et al.* [2008] estimated the effect of H_2O on Fo_{100} wadsleyite from Brillouin spectroscopy on samples containing 0.37–1.66 wt % H_2O and suggested 1 wt % H_2O causes a 7.6% decrease in K_{S0}. The fit to K_{S0} by *Mao et al.* [2008] was given as $K_{S0} = 170.9(9) - 13.0(8)C_{H2O}$, where C_{H2O} is the water content in weight percent. However, we note that the samples measured by *Mao et al.* [2008], namely, WH833, WH2120, and SS0401, are from the same synthesis runs that we have reanalyzed by NanoSIMS in the current study, showing considerably more H_2O in WH2120 and SS0401 than estimated by FTIR methods.

The effect of H_2O on the bulk modulus of Mg- and Fe-bearing wadsleyite is illustrated in Figure 11. We include data from both static compression (current study) and several previous Brillouin spectroscopy studies for comparison [*Mao et al.*, 2008, 2011; *Wang et al.*, 2014]. The relation between the adiabatic (K_{S0}) and isothermal (K_{T0}) bulk modulus is $K_T = K_S/(1+\gamma\alpha T)$; however, because the $1+\alpha\gamma T$ term is close to unity, for the purpose of the current discussion we will refer to K_{S0} and K_{T0} interchangeably as K_0. In Figure 11, the variation of K with water content is most steep for the Mg-wadsleyite data of *Mao et al.* [2008], with $dK_0/dC_{H2O} = -13.0(8)$ GPa/wt % H_2O. However, when we apply the new NanoSIMS H_2O contents measured in this study on samples from the same synthesis runs, the slope decreases dramatically to $dK_0/dC_{H2O} = -7.0(5)$ GPa/wt % H_2O (Figure 11). For Fe-bearing wadsleyite, including the anhydrous value from *Wang et al.* [2014], the two Fe-bearing samples from this study, and the Brillouin measurements of SZ0570 from *Mao et al.* [2011], we

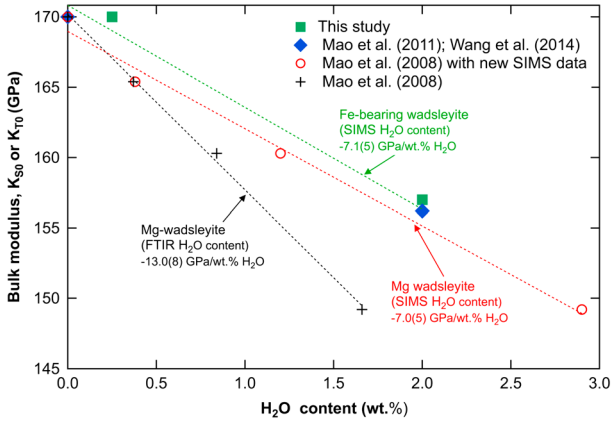

Figure 11. Bulk modulus (K_0) versus H_2O content for wadsleyite. The black dashed line represents the fitting result with FTIR H_2O content after *Mao et al.* [2008], and the red dashed line represents the new result with SIMS H_2O values. The bulk modulus versus H_2O relationship for Fe-bearing wadsleyite is presented by green dashed line fit to *Wang et al.* [2014], *Mao et al.* [2011], and the current study.

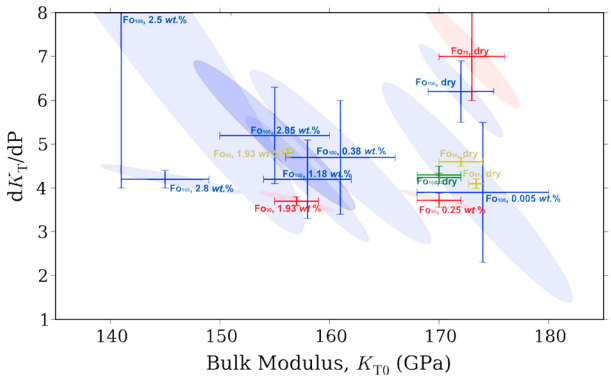

Figure 12. Confidence ellipsoids constructed from data sets obtained in this and previous studies. References used in this figure are listed in Table 6. The blue ellipses represent Mg end-member wadsleyite with different H_2O content. The red ellipses represent Fe-bearing wadsleyite with different H_2O content. The equations of state measured by sound velocity techniques are shown in deep and light green symbols.

obtain $dK_0/dC_{H2O} = -7.1(5)$ GPa/wt % H_2O. Thus, our new interpretation of all the data is that water influences the bulk modulus of Fe-free and Fe-bearing wadsleyite similarly, with an offset to slightly lower values for Fe-bearing samples due to Fe substitution for Mg.

In contrast to the consistent reduction in bulk modulus with increasing H_2O content across many experimental studies, the effect of H_2O on K_0' is not as systematic or straightforward (Figure 1). As noted earlier, reports range from 4 to >5 from different studies on similar compositions. Compressibility studies in particular have suggested elevated K_{T0}' for hydrous Mg-wadsleyite [*Holl et al*., 2008]. This was attributed to the repulsive force between oxygen atoms in the M3 vacancies. However, the current study using the comparative compressibility method on Fe-bearing wadsleyite does not show an effect of H_2O on K_0'. The K_{T0}' of Z0902 (0.25 wt % H_2O) is indistinguishable within mutual uncertainties from the K_{T0}' of Z0570 (2.0 wt % H_2O) in this study. Fitting the *P-V* data in XRD compression experiments suffers from a well-known correlation issue between fitted K and K_0'. In order to illustrate this correlation, we refitted the EOS of previously reported data and constructed confidence ellipses for each data set as shown in Figure 12. Reconstructing confidence ellipses of previous data allows us to compare not only the best fitting third-order BM equations of state but also the potential combinations of (K_{T0}, K_{T0}') which should fit the data equally well within the 63% confidence region (1σ) as the best fitting results. For comparison (Figure 12), results from sound velocity measurements were also converted to K_{T0} and K_{T0}' via thermodynamic relationships. Figure 12 demonstrates that the EOS is less well constrained in experiments with smaller pressure ranges, especially the value of K_{T0}' which is the second-order derivative of the *P-V* curve and strongly affected by the pressure range of data. The K_{T0}' for hydrous Mg-wadsleyite is best constrained in the experiment performed by *Ye et al*. [2010]. The observed range of K_{T0}' for a very hydrous Mg-wadsleyite (2.8 wt % H_2O) is between 4 and 5. Although *Holl et al*. [2008] suggested that increasing H_2O content elevates the value of K_{T0}', this is not clearly seen from this plot. The confidence ellipse of Z0570 is almost identical to the confidence ellipse of Z0902, only shifted to lower K_{T0}. This confirms that the combined influence of Fe and H_2O does not affect K_{T0}'. Therefore, more hydrated Fe-bearing wadsleyite becomes more compressible and remains more compressible than anhydrous wadsleyite at transition zone pressures.

3.3. Comparison of Static Compression and Sound Velocity Measurements

As shown in Figure 12, the bulk modulus of wadsleyite samples with similar compositions is consistent across various experimental studies. Despite the remarkable variation in K_0' between studies (Figure 1), values from acoustic measurements are regarded to be more reliable than K_0' fitted from *P-V* data because of the well-known correlation between K and K_0' (illustrated in Figure 12). The elastic properties of the hydrous Fe-bearing wadsleyite sample used in this study (run Z0570) were also studied by *Mao et al*. [2011] using Brillouin spectroscopy up to 12 GPa, allowing a direct comparison. The bulk modulus obtained from this study and *Mao et al*. [2011] is consistent within mutual uncertainties (Table 6). However, the K_0' from *Mao et al*. [2011] of 4.8(1) falls considerably outside the confidence ellipse of the sample Z0570 in this study with $K_0' = 3.8(1)$ (Figure 12). This suggests that these two data sets are incompatible. In order to examine the source of the discrepancy in K_0' between our study and *Mao et al*. [2011], we compared the V/V_0 ratios at high pressures in the two experiments. The V/V_0 ratio in the sound velocity measurement was calculated from the ρ_0/ρ ratio, where density ρ_0 was calculated using the measured V_0, and ρ values at high pressures were estimated via a "self-consistent method" [*Mao et al*., 2011]. In this method, an initial density model was used to obtain K_{S0} and K_{S0}' from a least square fit to the finite strain

Table 6. Compilation of Equation of State Data for Wadsleyite and Ringwoodite[a]

	X_{Fe}	H_2O (wt %)	K_0 (GPa)	$K_0' = (dK/dP)_{P=0}$	Method[b]	P_{max} (GPa), T_{max} (K)	References
Anhy-wadsleyite	0	0	170(2)	4.24(10)	UI	12.5, RT	(1)
	0	0	169.2 (fixed)	4.1(1)	XRD	20, 2100	(2)
	0	0	170(2)	4.3(2)	BS	14, RT	(3)
	0	0	172(3)	6.3(7)	XRD	10.12, RT	(4)
	0.075	0	170(3)	4.1(1)	BS	17.7, RT	(17)
	0.12	0	172(3)	4.6(1)	UI	10, RT	(5)
	0.13	0	175.4(7)	4.10(11)	UI	12, 1073	(6)
	0.13	0	171.3(fixed)	4.74(8)	UI	12, 1073	(6)
	0.16	0	174(3)	4.0(fixed)	XRD	26, 900	(12)
	0.25	0	173(3)	7.1(8)	XRD	10.12, RT	(4)
Hyd-wadsleyite	0	0.005	173(5)	4.1(15)	XRD	7.3, RT	(7)
	0	0.37 (0.38[c])	161(4)	5.4(11)	XRD	9.01, RT	(7)
	0	0.37 (0.38[c])	165.4(9)	--	BS	Ambient	(8)
	0	0.84 (1.20[c])	160.3(7)	--	BS	Ambient	(8)
	0	1.18	158(4)	4.2(9)	XRD	8.56, RT	(7)
	0	1.66 (2.9[c])	154(4)	4.9(11)	XRD	9.58, RT	(7)
	0	1.66 (2.9[c])	149.2(6)	--	BS	Ambient	(8)
	0	2.5	155(2)	4.3(fixed)	XRD	8.5, RT	(9)
	0	2.8	137(5)	4.5(3)	XRD	60, RT	(10)
	0.10	0.25	170(2)	3.72(16)	XRD	31.9, RT	This study
	0.11	1.93 (2.0[c])	156.2(5)	4.8(1)	BS	12, RT	(11)
	0.11	1.93 (2.0[c])	157(2)	3.77(14)	XRD	31.9, RT	This study
Ringwoodite	0.09	0	188(3)	4.1(3)	BS	16, 923	(13)
	0.11	0.89	177(4)	5.3(4)	UI	9, RT	(14)
	0.11	0.79	175(3)	6.2(6)	XRD	45, RT	(15)
	0.14	1.1	175(1)	4.0(1)	BS	16, 673	(16)
	0.17	1.38	177(3)	3.7(2)	XRD	31.9, RT	This study

[a]References: (1) *Li and Gwanmesia*, [1996], (2) *Katsura et al.* [2009], (3) *Zha et al.* [1997], (4) *Hazen et al.* [2000a], (5) *Li and Liebermann* [2000], (6) *Liu et al.* [2009], (7) *Holl et al.* [2008], (8) *Mao et al.* [2008], (9) *Yusa and Inoue* [1997], (10) *Ye et al.* [2010], (11) *Mao et al.* [2011], (12) *Fei et al.* [1992], (13) *Sinogeikin et al.*, [2003], (14) *Jacobsen and Smyth* [2006], (15) *Manghnani et al.* [2005], (16) *Mao et al.* [2012], and (17) *Wang et al.* [2014].
[b]Methods: UI, ultrasonic interferometry; BS, Brillouin scattering; XRD, X-ray diffraction.
[c]H_2O content remeasured by SIMS (this study).

equation. The measured adiabatic bulk modulus is converted to isothermal bulk modulus (K_T) at various pressures to construct the isothermal compression curve. The densities at high-pressure conditions are then determined using the isothermal compression curve and the initial density. The results of V/V_0 versus P from both experiments are plotted together in Figure 13 and show a good agreement between data sets. We therefore conclude that the discrepancy in K_0' is likely to have been introduced by the numerical fitting processes.

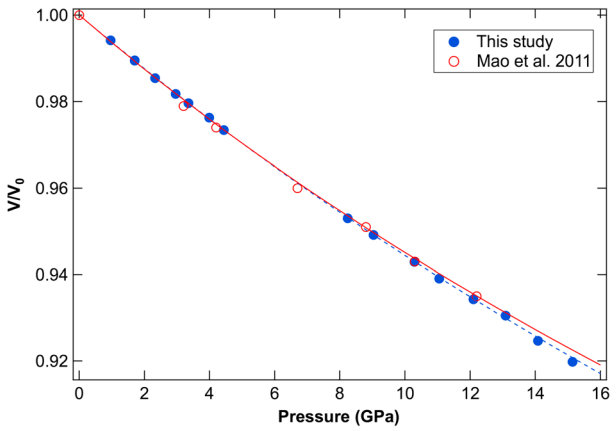

Figure 13. Normalized volume (V/V_0, where V_0 is the initial volume) for hydrous Fe-bearing wadsleyite (Z0570, filled symbols, this study) and calculated from the density ratio from *Mao et al.* [2011], red open circles.

Bass et al. [1981] found that when the value of K_{T0} yielded by the compression data is compatible with the acoustically determined values within the mutual uncertainties, the accuracy of K_{T0}' obtained in a *P-V* data set can be improved by fixing K_{T0} at the acoustically determined value in the least squares calculation. We therefore refit the compression data with K_{T0} constrained at the acoustically determined value by *Mao et al.* [2011] and refined only V_0 and K_{T0}'. The resulting value of K_{T0}' is 3.88(4), which is in excellent agreement with our original result $K_0' = 3.77(14)$. The resulting V_0 is also consistent with the V_0 in our original third-order BM equation of state. It can be seen in Figure 13 that

the two V/V_0 versus P curves calculated from the EOS of the two experiments deviate from each other above 12 GPa, while the data points at ~12 GPa from two experiments are still in good agreement with each other. As shown in Figure 12, K_{T0}' is the second-order derivative of the P-V curve and especially sensitive to the pressure range over which data are obtained. We consider the potential influence of pressure range on K_{T0}' and refit the compression data only to 12 GPa; the resulting K_{T0}' is 4.16(14), still in reasonable agreement with the original result. The elevated K_{S0}' in the acoustic measurement is possibly affected by the slightly higher V/V_0 ratio at ~12 GPa, and the lack of constraints at higher pressures. Scanning through our fitting results with various pressure ranges and methods, a K_{T0}' value close to 4.0(0.2) is robust and may be a good assumption for a Fo_{90}-wadsleyite, in excellent agreement with the recent results for $K_{S0}' = 4.1(1)$ from *Wang et al.* [2014]. The discrepancies in K_0' between the XRD and acoustic measurements are more likely rooted in the calibration and fitting methods across experiments than in the physical properties of samples. Regardless of the uncertain absolute value of K_0', both *Mao et al.* [2011] and our study conclude that hydration has no effect on the K_0' of Fe-bearing wadsleyite. A similar absence of effect of hydration on K_0' of Fe-bearing olivine was also suggested by *Chen et al.* [2011].

3.4. Influence of dK/dP on Bulk Sound Velocity in the Transition Zone

Comparison between sound velocities derived from mineralogical models and observed seismic velocity is potentially an important tool for constraining the hydration state of the transition zone. In order to demonstrate the importance and influence of K_0' on the predicted sound velocity of wadsleyite, the bulk sound velocity ($V_\Phi = [K/\rho]^{1/2}$) of anhydrous and hydrous Fe-bearing (Fo_{90}) wadsleyite was calculated using two self-consistent data sets (Table 7); one using $K_0' = 3.8$ implied form the current study and one using $K_0' = 4.8$ implied from the study of *Mao et al.* [2011]. The bulk sound velocity gradient for the $K_0' = 3.8$ data set is 1.72 (m/s/km) for anhydrous wadsleyite and 1.81 m/s/km for hydrous wadsleyite in the depth range 410–520 km (Figure 14). Raising K_0' from 3.8 to 4.8 increases the velocity gradient by about 0.55 m/s/km, or about 30%, for both dry and hydrous wadsleyite. As shown in the current study, the effect of hydration on the velocity gradient in the wadsleyite-rich part of the transition zone is not expected to be significant due to the minimal effect of H_2O on K_0' (whether or not ~4 or ~5 is used). Instead, the major effect of hydration on Fe-bearing wadsleyite will be the reduction in sound velocities associated with the ~7 GPa/wt % H_2O reduction in the bulk modulus, shown in Figure 11. Whether K_0' ~4 or ~5 is assumed, the difference in bulk sound velocity between anhydrous and hydrous wadsleyite is around 200 m/s, or 2.5%, at transition zone conditions (Figure 14). Accordingly, the expected reduction in bulk sound velocity in very hydrous regions of the transition zone would be around 1.5% in pyrolite (60% olivine component), which is potentially detectible seismically in high-resolution, regional studies.

In contrast to hydrous versus anhydrous olivine (Fo_{100}) [*Mao et al.*, 2010], comparing the bulk sound velocities of anhydrous and hydrous Fe-bearing wadsleyite (Fo_{90}), no velocity crossover was observed in either the $K_0' = 3.8$ or the $K_0' = 4.8$ data sets. The differences in velocities between anhydrous and hydrous Fe-bearing wadsleyite are about 175 m/s (2.5%) and 165 m/s (2.2%) at 1673 K for $K_0' = 3.8$ and $K_0' = 4.8$, respectively. These differences remain essentially constant in the depth range 410–520 km for both cases. However, if we remove the constraint imposed from this study that K_0' of anhydrous and hydrous wadsleyite are similar and instead compare V_Φ for anhydrous wadsleyite with K_0' ~4 [*Katsura et al.*, 2009; *Wang et al.*, 2014] and V_Φ for hydrous wadsleyite with $K_0' = $ ~5 [*Holl et al.*, 2008; *Mao et al.*, 2011], a velocity crossover occurs at a depth of ~350 km, implying that hydrous wadsleyite would be the faster phase at transition zone pressures, which seems highly unlikely.

The importance of constraining K_0' also becomes evident in attempting to estimate of the fraction of olivine in Earth's mantle. Assuming the Fe content in olivine and wadsleyite in the Earth's mantle is about 10 mol % and H_2O partitioning of 1:5 between olivine and wadsleyite [*Inoue et al.*, 2010], the contrast in bulk sound velocity ($\Delta V_{\alpha-\beta}$) at 410 km along a 1673 K adiabat calculated with thermal parameters in Table 7 and using $K_0 = 123(3)$ GPa and $K_0' = 4.6$ for 0.4 wt % H_2O Fe-bearing olivine (Fo_{90}) [*Chen et al.*, 2011], we obtain $\Delta V_{\alpha-\beta} = 4.7\%$ against hydrous wadsleyite with $K_0' = 3.8$ and $\Delta V_{\alpha-\beta} = 8.1\%$ when $K_0' = 4.8$ is used. As a consequence, the bulk sound velocity contrast of 3.3% used in the IASP91 model [*Kennett and Engdahl*, 1991] would correspond to around 70% olivine under hydrous conditions when $K_0' = 3.8$ is used, but only 40% olivine if $K_0' = 4.8$ is used. A similar wide range of possible results is obtained for dry conditions (dry moduli for olivine and wadsleyite), yielding ~60% olivine when $K_0' = 3.8$ is used for anhydrous wadsleyite and ~37%

Table 7. Thermoelastic Data Sets Used to Compare Bulk Sound Velocity in the Transition Zone Under Anhydrous (Anhy) and Hydrous (Hyd) Conditions for Various Scenarios of K_0' Discussed in the Text[a]

	K_{S0} (GPa)[b]	K_{S0}'	ρ_0 (g/cm^3)	dK_S/dT (GPa K^{-1})	$\alpha \times 10^{-5}$ (K^{-1})	Reference
			Data Set 1			
Anhy-wadsleyite	172(2)	3.72(16)	3.600	−0.0170	3.40	d
Hyd-wadsleyite	158(2)	3.77(14)	3.520	−0.0170	3.40	d
Anhy-olivine	129(4)	4.6(fixed)	3.351[c]	−0.0175	3.64	e
Hyd-olivine	124(3)	4.6(fixed)	3.331[c]	−0.0175	3.64	e
			Data Set 2			
Anhy-wadsleyite	171.3(fixed)	4.74(8)	3.633	−0.0170	3.40	f
Hyd-wadsleyite	156.2(5)	4.8(1)	3.520	−0.0170	3.40	g
Anhy-olivine	131.1(1.9)	3.8(2)	3.343	−0.0175	3.64	h
Hyd-olivine	124(3)	3.8(2)	3.331	−0.0175	3.64	i

[a]For hydrous conditions, 0.4 wt % H_2O in olivine and 2.0 wt % H_2O in wadsleyite are used.
[b]K_{T0} from this study and *Chen et al.* [2011] were converted to K_{S0} using $K_{S0}/K_{T0} = 1.01$.
[c]Calculated using the chemical compositions and V_0 from *Chen et al.* [2011].
[d]This study, *Liu et al.* [2009], and *Inoue et al.* [2004].
[e]*Chen et al.* [2011], *Liu and Li*, [2006], *Isaak et al.* [2010], and *Ye et al.* [2009].
[f]*Liu et al.* [2009] and *Inoue et al.* [2004].
[g]*Mao et al.* [2011], *Liu et al.* [2009], and *Inoue et al.* [2004].
[h]*Mao et al.* [2011], *Liu et al.* [2009], and *Inoue et al.* [2004].
[i]K_{S0} from *Chen et al.* [2011]; K_{S0}' assumed equal to Anhy-olivine.

when $K_0' = 4.8$ is used. Further, if K_0' of Fe-bearing olivine is reduced from 4.6 to 3.8, using a value of $K_0 = 130$ GPa (Table 7) would give 38% and 28% olivine fraction when $K_0' = 3.8$ and 4.8 for wadsleyite, respectively. However, the olivine fraction estimated using the self-consistent data sets (Table 7) is ~40% for both dry and hydrous conditions. Here we have demonstrated how it would be nearly impossible to accurately estimate the olivine fraction of the mantle near 410 km without better experimental constraints on K_0'.

In this study, we also constrain the relative value of K_0' between Fe-bearing hydrous wadsleyite (Fo_{90}) and ringwoodite (Fo_{83}). The resulting K_0' of hydrous Fo_{83} ringwoodite ($X_{Fe} = 0.17$, 1.38 wt % H_2O) is 3.7(2), which is indistinguishable from the $K_0' = 3.77(14)$ of the coexisting Fo_{90} wadsleyite. The reported K_0' of hydrous Fe-bearing ringwoodite from previous studies ranges from 4.0(1) to 6.2(6) (Table 5 and Figure 15). We stress that in this study, we are more focused on accurately constraining the possible change in K_0' with composition (specifically, H_2O content) and structure (between hydrous wadsleyite and hydrous ringwoodite), rather than on absolute values, which are subject to statistical trade-off with K_0 in *P-V* fitting studies, as discussed above. *Mao et al.* [2012] suggested that hydration does not affect K_0' of Fe-bearing ringwoodite. The reported $K_0' = 4.0(1)$ of a Fo_{89} ringwoodite (1.1 wt % H_2O) in *Mao et al.* [2012] is indistinguishable from $K_0' = 4.1(3)$ reported for dry Fo_{91} ringwoodite [*Sinogeikin et al.*, 2003]. The values of K_0' ~4.0 for dry and hydrous Fe-bearing ringwoodite from Brillouin scattering [*Mao et al.*, 2012; *Sinogeikin et al.*, 2003] are significantly lower than the reported $K_0' = 4.8(1)$ of hydrous Fo_{90}-wadsleyite *from Mao et al.* [2011], implying a difference of 20% between K_0' of hydrous wadsleyite and hydrous ringwoodite. Ultrasonic measurements by *Jacobsen and Smyth* [2006] reported an extremely elevated $K_{S0}' = 5.3(4)$ for hydrous Fo_{89} ringwoodite (0.89 wt % H_2O). We have found through comparative compressibility studies that the difference between K_0' of hydrous wadsleyite and hydrous ringwoodite is indistinguishable.

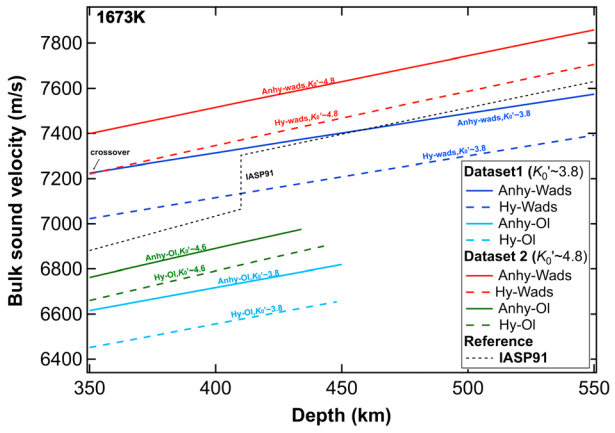

Figure 14. Comparison of bulk sound velocities for dry and hydrous phases along a 1673 K adiabat using $K_0' = 3.8$ and $K_0' = 4.8$. Data sets 1 and 2 are defined in Table 7.

Next we compare the calculated bulk sound velocity jump between wadsleyite and ringwoodite ($\Delta V_{\beta-\gamma}$) at transition

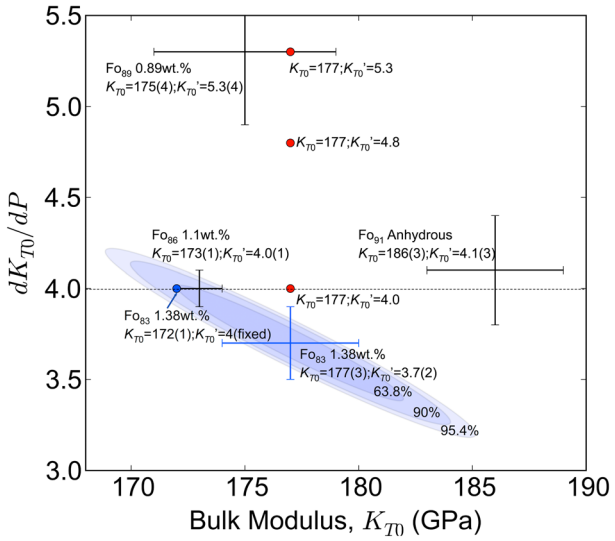

Figure 15. Confidence ellipsoids calculated from the equation of state fit for ringwoodite (Z0570) in this study. References for Fe-bearing ringwoodite used in this figure are listed in Table 6. The blue dot represents the result of a second-order BM equation of state for ringwoodite (Z0570). The equations of state measured by sound velocity techniques are converted to isothermal bulk moduli using the thermodynamic relationship in the text. The red dots represent the hypothetical equations of state used in Figure 15 to illustrate the effect of K_0' ranging from 4 to 5.3.

zone pressures for cases in which K_0' of Fe-bearing ringwoodite is higher, equal, and lower than the K_0' of Fe-bearing wadsleyite. The equations of state for hydrous Fe-bearing wadsleyite (Z0570) from this study and *Mao et al.* [2011] were used in these calculations. For hydrous Fe-bearing ringwoodite, we used the K_0 of ringwoodite (Z0570) from this study and varied K_0' from 4.0 to 5.3 to reflect the published range, as shown by the red dots in Figure 15. The bulk sound velocity jump ($\Delta V_{\beta-\gamma}$) calculated at 300 K using the measured equations of state for coexisting wadsleyite and ringwoodite in this study is ~2.2% (Figure 16), corresponding to about 1.3% contrast for a 60% $(Mg,Fe)_2SiO_4$ mantle component. If a value of $K_0'=4.8$ for hydrous wadsleyite is used [*Mao et al.*, 2011], the bulk sound velocity contrast with ringwoodite ($\Delta V_{\beta-\gamma}$) ranges from −0.16% to 4.3% as K_0' of hydrous ringwoodite varies from 4.0 to 5.3 (Figure 16). However, when we force the K_0' of hydrous wadsleyite and hydrous ringwoodite to be the same as found in this study (either 3.8 or 4.8), the resulting $\Delta V_{\beta-\gamma}$ is consistently around 2.7% (or 1.6% for 60% olivine component in pyrolite), consistent with the current experimental results. Whereas the absolute values of K_0' remain uncertain, the very tight constraint on the relative values of K_0' between phases from this study provide a very reasonable estimation for the predicted velocity jump at 520 km of around 1.5% under dry or hydrous conditions.

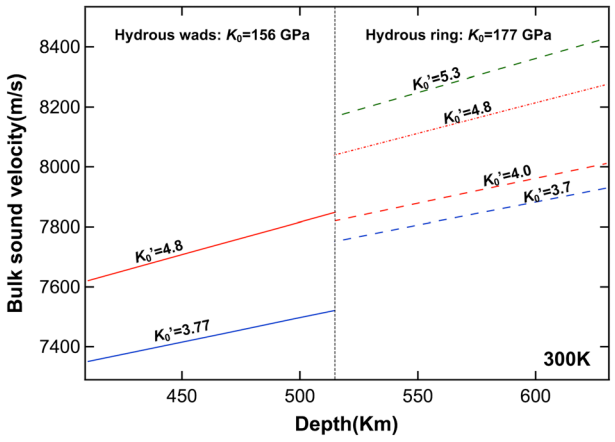

Figure 16. Comparison of bulk sound velocity jumps between hydrous wadsleyite and hydrous ringwoodite ($\Delta V_{\beta-\gamma}$) calculated at 300 K using $K_0 = 156$ GPa for wadsleyite and $K_0 = 175$ GPa for ringwoodite, with various reported values of K_0' for ringwoodite. The $\Delta V_{\beta-\gamma}$ calculated from this study is ~2.2%. The $\Delta V_{\beta-\gamma}$ varies from −0.16% to 4.3% using values of K_0' that span the experimental literature. In the current study, we find no difference between K_0' of hydrous wadsleyite and hydrous ringwoodite, so for either K_0' ~4 or ~5, the contrast is around 2.5% for wadsleyite, 1.5% for a transition zone composition of 60% olivine component.

4. Conclusions

Consistent trends for the effect of Fe and H_2O on K_0 for wadsleyite and ringwoodite are in contrast to widely scattered values of K_0' found in recent experimental studies. Here we have discussed the importance of constraining K_0', if only the difference in K_0', between compositions and structures of Mg_2SiO_4. Comparing the bulk sound velocity (V_Φ) of hydrous wadsleyite calculated with K_0' ~4 versus K_0' ~5 at a depth of 410 km results in a 230 m/s difference (3.3%), which is comparable to the velocity reduction caused by ~2 wt % H_2O in wadsleyite. Therefore, it is not feasible to accurately constrain the bulk mantle water content from current mineral physics equations of state parameters owing to the lack of consensus on K_0'. In this study, we provide strong evidence through comparative

compressibility studies that water does not influence K_0', leaving the majority of influence expressed in reductions of K_0. We have revisited the composition of hydrous wadsleyite samples from a number of previous studies using SIMS and, in combination with the current results, revised estimates for the influence of H_2O on wadsleyite K_0 from about −13 GPa/wt % H_2O [e.g., *Mao et al*., 2008] to −7 GPa/wt % H_2O for both Mg- and Fe-bearing wadsleyite. The absolute value of K_0' from *P-V* or acoustic methods is strongly affected by the numerical analysis and fitting processes. The resulting values of K_0' from recent studies are scattered even when the experimental data sets are consistent with each other, as we have demonstrated in this study. A more consistent data processing method across differing experimental techniques is needed for future studies.

Acknowledgments

This research was supported by grants from National Science Foundation (NSF) EAR-0748707 and EAR-1452344, the Carnegie/DOE Alliance Center (CDAC), the David and Lucile Packard Foundation, and by the Alexander von Humboldt Foundation to S.D. Jacobsen. Support was also provided by NSF grants EAR-1344942 and EAR-1440005 to P. Dera, EAR-11-13369 to J.R. Smyth, and EAR-1215957 and EAR-1417274 to S.M. Thomas. Portions of this work were performed at HPCAT (Sector16) of the Advanced Photon Source (APS), Argonne National Laboratory. HPCAT operations are supported by DOE-NNSA under award DE-NA0001974 and DOE-BES under award DE-FG02-99ER45775, with partial instrumentation funding from NSF. Use of the COMPRES-GSECARS gas loading system was supported by COMPRES under NSF Cooperative Agreement EAR11-57758 and by GSECARS through NSF grant EAR-1128799 and DOE grant DE-FG02-94ER14466. Use of the APS was supported by the U.S. Department of Energy, Office of Science, Office of Basic Energy Sciences, contract DE-AC02-06CH11357. All of the numerical information used in this study is provided in the figures and tables.

References

Angel, R. J., and L. W. Finger (2011), Single: A program to control single-crystal diffractometers, *J. Appl. Crystallogr.*, *44*, 247–251.

Angel, R. J., D. R. Allan, R. Miletich, and L. W. Finger (1997), The use of quartz as an internal pressure standard in high-pressure crystallography, *J. Appl. Crystallogr.*, *30*, 461–466.

Angel, R. J., J. Gonzales-Platas, and M. Alvaro (2014), EosFit7c and a Fortran module (library) for equation of state calculations, *Z Kristallogr.*, *229*, 405–419.

Bass, J. D., R. C. Liebermann, D. J. Weidner, and S. J. Finch (1981), Elastic properties from acoustic and volume compression experiments, *Phys. Earth Planet. Int.*, *25*, 140–158.

Bell, P. M., H. -K. Mao, and J. A. Xu (1987), Error analysis of parameter-fitting in equations of state for mantle minerals, in *High-pressure Research in Mineral Physics*, edited by M. H. Manghnani and Y. Syono, pp. 447–454, Terra Scientific, Tokyo, Washington, D. C.

Bevington, P. R. (1969), *Data Reduction and Error Analysis for the Physical Sciences*, McGraw-Hill, New York.

Bina, C. R. (1995), Confidence limits for silicate perovskite equations of state, *Phys. Chem. Min.*, *22*, 375–382.

Bina, C. R., and G. Helffrich (1994), Phase transition Clapeyron slopes and transition zone seismic discontinuity topography, *J. Geophys. Res.*, *99*, 15,853–15,860, doi:10.1029/94JB00462.

Birch, F. (1952), Elasticity and constitution of the Earth's interior, *J. Geophys. Res.*, *57*, 227–285, doi:10.1029/JZ057i002p00227.

Bolfan-Casanova, N., H. Keppler, and D. C. Rubie (2000), Water partitioning between nominally anhydrous minerals in the MgO-SiO_2-H_2O system up to 24 GPa: Implications for the distribution of water in the Earth's mantle, *Earth Planet. Sci. Lett.*, *182*, 209–211.

Bolfan-Casanova, N., M. Muñoz, C. A. McCammon, E. Deloule, A. Férot, S. Demouchy, L. France, D. Andrault, and S. Pascarelli (2012), Ferric iron and water incorporation in wadsleyite under hydrous and oxidizing conditions: A XANES, Mossbauer, and SIMS study, *Am. Mineral.*, *97*, 1483–1493.

Chen, J., H. Liu, and J. Girard (2011), Comparative in situ X-ray diffraction study of San Carlos olivine: Influence of water on the 410 km seismic velocity jump in Earth's mantle, *Am. Mineral.*, *96*, 697–702.

Demouchy, S., E. Deloule, D. J. Frost, and H. Keppler (2005), Pressure and temperature-dependence of water solubility in Fe-free wadsleyite, *Am. Mineral.*, *90*, 1084–1091.

Deon, F., M. Koch-Müller, D. Rhede, M. Gottschalk, R. Wirth, and S.-M. Thomas (2010), Location and quantification of hydroxyl in wadsleyite: New insights, *Am. Mineral.*, *95*, 312–322.

Dera, P. (2007a), *GSE-ADA Data Analysis Program for Monochromatic Single Crystal Diffraction with Area Detector*, GeoSoilEnviroCARS, Argonne, Ill.

Dera, P. (2007b), *RSV Reciprocal Space Viewer Program for Single Crystal Data Analysis*, GeoSoilEnviroCARS, Argonne, Ill.

Dewaele, A., F. Datchi, and P. Loubeyre (2008), High pressure–high temperature equations of state of neon and diamond, *Phys. Rev. B.*, *B77*, 094106.

Dorogokupets, P. I. (2010), P-V-T equations of state of MgO and thermodynamics, *Phys. Chem. Miner.*, *37*, 677–684.

Duffy, T., and D. Anderson (1989), Seismic velocities in mantle minerals and the mineralogy of the upper mantle, *J. Geophys. Res.*, *B2*, 1895–1912, doi:10.1029/JB094iB02p01895.

Fei, Y., H. K. Mao, J. Shu, G. Parthasarathy, W. A. Bassett, and J. Ko (1992), Simultaneous high-*P*, high-*T* X ray diffraction study of β-$(Mg,Fe)_2SiO_4$ to 26 GPa and 900 K, *J. Geophys. Res.*, *97*, 4489–4495, doi:10.1029/92JB00076.

Finger, L., R. Hazen, J. Zhang, and J. Ko (1993), The effect of Fe on the crystal structure of wadsleyite β-$(Mg_{1-x}Fe_x)_2SiO_4$, $0.00 \le x \le 0.40$, *Phys. Chem. Miner.*, *19*, 361–368.

Frost, D. (2003), The structure and sharpness of $(Mg, Fe)_2SiO_4$ phase transformations in the transition zone, *Earth Planet. Sci. Lett.*, *216*, 313–328.

Griffin, J. M., A. J. Berry, D. J. Frost, S. Wimperis, and S. E. Ashbrook (2013), Water in the Earth's mantle: A solid-state NMR study of hydrous wadsleyite, *Chem. Sci.*, *4*, 1523–1538.

Gwanmesia, G. D., R. C. Liebermann, and F. Guyot (1990), Hot-pressing and characterization of polycrystals of beta-Mg_2SiO_4 for acoustic velocity measurements, *Geophys. Res. Lett.*, *17*, 1331–1334, doi:10.1029/GL017i009p01331.

Hauri, E. H., A. M. Shaw, J. Wang, J. E. Dixon, P. L. King, and C. Mandeville (2006), Matrix effects in hydrogen isotope analysis of silicate glasses by SIMS, *Chem. Geol.*, *225*, 352–365.

Hazen, R. M., M. B. Weinberger, H. X. Yang, and C. T. Prewitt (2000a), Comparative high-pressure crystal chemistry of wadsleyite, beta-$(Mg_{1-x}Fe_x)_2SiO_4$, with $x = 0$ and 0.25, *Am. Mineral.*, *85*, 770–777.

Hazen, R. M., H. X. Yang, and C. T. Prewitt (2000b), High-pressure crystal chemistry of Fe^{3+}-wadsleyite, beta-$Fe_{2.33}Si_{0.67}O_4$, *Am. Mineral.*, *85*, 778–783.

Holl, C. M., J. R. Smyth, S. D. Jacobsen, and D. J. Frost (2008), Effects of hydration on the structure and compressibility of wadsleyite, β-(Mg_2SiO_4), *Am. Mineral.*, *93*, 598–607.

Holland, T., and S. Redfern (1997), Unit cell refinement from powder diffraction data: The use of regression diagnostics, *Mineral. Mag.*, *61*, 65.

Inoue, T., H. Yurimoto, and Y. Kudoh (1995), Hydrous modified spinel, $Mg_{1.75}SiH_{0.5}O_4$: A new water reservoir in the mantle transition region, *Geophys. Res. Lett.*, *22*, 117–120, doi:10.1029/94GL02965.

Inoue, T., Y. Tanimoto, T. Irifune, T. Suzuki, H. Fukui, and O. Ohtaka (2004), Thermal expansion of wadsleyite, ringwoodite, hydrous wadsleyite and hydrous ringwoodite, *Phys. Earth Planet. Int.*, *143–144*, 279–290.

Inoue, T., T. Wada, R. Sasaki, and H. Yurimoto (2010), Water partitioning in the Earth's mantle, *Phys. Earth Planet. Int.*, *183*, 245–251.
Irifune, T., and M. Isshiki (1998), Iron partitioning in a pyrolite mantle and the nature of the 410-km seismic discontinuty, *Nature*, *392*, 702–705.
Irifune, T., and A. E. Ringwood (1987), Phase-transformations in a harzburgite composition to 26 GPa—Implications for dynamical behavior of the subducting slab, *Earth Planet. Sci. Lett.*, *86*, 365–376.
Isaak, D. G., G. D. Gwanmesia, M. G. Davis, S. C. Stafford, A. M. Stafford, and R. S. Triplett (2010), The temperature dependence of the elasticity of Fe-bearing wadsleyite, *Phys. Earth Planet. Int.*, *182*, 107–112.
Jacobsen, S. D. (2006), Effect of water on the equation of state of nominally anhydrous minerals, *Rev. Mineral. Geochem.*, *62*, 321–342.
Jacobsen, S. D., and J. R. Smyth (2006), Effect of water on the sound velocities of ringwoodite in the transition zone, in *Earth's Deep Water Cycle*, *Geophys. Monogr. Ser.*, vol. 168, edited by S. D. Jacobsen and S. van der Lee, pp. 131–145.
Jacobsen, S. D., S. Demouchy, D. J. Frost, T. Boffa Ballaran, and J. Kung (2005), A systematic study of OH in hydrous wadsleyite from polarized FTIR spectroscopy and single-crystal X-ray diffraction: Oxygen sites for hydrogen storage in Earth's interior, *Am. Mineral.*, *90*, 61–70.
Jacobsen, S. D., C. M. Holl, K. A. Adams, R. A. Fischer, E. S. Martin, C. R. Bina, J.-F. Lin, V. B. Prakapenka, A. Kubo, and P. Dera (2008), Compression of single-crystal magnesium oxide to 118 GPa and a ruby pressure gauge for helium pressure media, *Am. Mineral.*, *35*, 1823–1828.
Jaocbsen, S. D., H. Reichmann, H. A. Spetzler, S. J. Macwell, J. R. Smyth, R. J. Angel, and C. A. McCammon (2002), Structure and elasticity of single-crystal (Mg, Fe)O and a new method of generating shear wave for gigahertz ultrasonic interferometry, *J. Geophys. Res.*, *107*(B2), 2037, doi:10.1029/2001JB000490.
Katsura, T., et al. (2009), *P-V-T* relations of wadsleyite determined by in situ X-ray diffraction in a large-volume high-pressure apparatus, *Geophys. Res. Lett.*, *36*, L113087, doi:10.1029/2009GL038107.
Kennett, B. L. N., and E. R. Engdahl (1991), Traveltimes for global earthquake location and phase identification, *Geophys. J. Int.*, *105*, 429–465.
Kennett, B. L. N., and I. Jackson (2009), Optimal equations of state for mantle minerals from simultaneous non-linear inversion of multiple datasets, *Phys. Earth Planet. Int.*, *176*, 98–108.
Kohlstedt, D. L., H. Keppler, and D. C. Rubie (1996), Solubility of water in the α, β, and γ phases of (Mg, Fe)$_2$SiO$_4$, *Contrib. Mineral. Petrol.*, *123*, 345–357.
Kudoh, Y., T. Inoue, and H. Arashi (1996), Structure and crystal chemistry of hydrous wadsleyite, $Mg_{1.75}SiH_{0.5}O_4$: Possible hydrous magnesium silicate in the mantle transition zone, *Phys. Chem. Miner.*, *23*, 461–469.
Li, B., and G. Gwanmesia (1996), Sound velocities of olivine and beta polymorphs of Mg_2SiO_4 at Earth's transition zone pressures, *Geophys. Res. Lett.*, *23*(17), 2259–2262, doi:10.1029/96GL02084.
Li, B. S., and R. C. Liebermann (2000), Sound velocities of wadsleyite beta-$(Mg_{0.88}Fe_{0.12})_2SiO_4$ to 10 GPa, *Am. Mineral.*, *85*, 292–295.
Li, B. S., and R. C. Liebermann (2007), Indor seismology by probing the Earth's interior by using sound velocity measurements at high pressures and temperatures, *Proc. Natl. Acad. Sci. U.S.A.*, *104*, 9145–9150.
Libowitzky, E., and G. R. Rossman (1997), An IR absorption calibration for water in minerals, *Am. Mineral.*, *82*, 1111–1115.
Liu, W., and B. Li (2006), Thermal equation of state of $(Mg_{0.9}Fe_{0.1})_2SiO_4$ olivine, *Phys. Earth Planet. Int.*, *157*, 188–195.
Liu, W., J. Kung, B. Li, N. Nishiyama, and Y. Wang (2009), Elasticity of $(Mg_{0.87}Fe_{0.13})_2SiO_4$ wadsleyite to 12 GPa and 1073 K, *Phys. Earth Planet. Int.*, *174*, 98–104.
Liu, W., L. Tian, and J. Zhao (2012), Water effects on high-pressure elasticity of olivine, wadsleyite and ringwoodite in Mg_2SiO_4 by first-principles, *Int. J. Mod. Phys. B*, *26*(19), 1250106.
Manghnani, M. H., G. Amulele, J. R. Smyth, C. M. Holl, G. Chen, V. Prakaprnka, and D. J. Frost (2005), Equation of state of hydrous Fo_{90} ringwoodite to 45 GPa by synchrotron power diffraction, *Mineral. Mag.*, *69*, 317–323.
Mao, Z., S. D. Jacobsen, F. Jiang, J. R. Smyth, C. M. Holl, D. J. Frost, and T. S. Duffy (2008), Single-crystal elasticity of wadsleyites, β-Mg_2SiO_4, containing 0.37–1.66 wt % H_2O, *Earth Planet. Sci. Lett.*, *266*, 78–89.
Mao, Z., S. D. Jacobsen, F. Jiang, J. R. Smyth, C. M. Holl, D. J. Frost, and T. S. Duffy (2010), Velocity crossover between hydrous and anhydrous forsterite at high pressures, *Earth Planet. Sci. Lett.*, *293*, 250–258.
Mao, Z., S. D. Jacobsen, D. J. Frost, C. A. McCammon, E. H. Hauri, and T. S. Duffy (2011), Effect of hydration on the single-crystal elasticity of Fe-bearing wadsleyite to 12 GPa, *Am. Mineral.*, *96*, 1606–1612.
Mao, Z., J.-F. Lin, S. D. Jacobsen, T. S. Duffy, Y.-Y. Chang, J. R. Smyth, D. J. Frost, E. H. Hauri, and V. B. Prakapenka (2012), Sound velocities of hydrous ringwoodite to 16 GPa and 673 K, *Earth Planet. Sci. Lett.*, *331–332*, 112–119.
McCammon, C., D. J. Frost, and J. R. Smyth (2004), Oxidation state of iron in hydrous mantle phases: Implications for subduction and mantle oxygen fugacity, *Phys. Earth Planet. Int.*, *143–144*, 157–169.
Miyagi, I., O. Matsubaya, and S. Nakashima (1998), Change in D/H ratio, water content and color during dehydration of hornblende, *Geochem. J.*, *32*, 33–48.
Mukherjee, D., K. D. Joshi, and S. C. Gupta (2013), High pressure equation of state and ideal compressive and tensile strength of MgO single crystal: Ab-initio calculations, *J. Appl. Phys.*, *113*, 233504.
Paterson, M. (1982), The determination of hydroxyl by infrared absorption in quartz, silicate glasses, and similar materials, *Bull. Mineral.*, *105*, 20–29.
Pearson, D. G., et al. (2014), Hydrous mantle transition zone indicated by ringwoodite included within diamond, *Nature*, *507*, 221–224.
Ringwood, A. E., and A. Major (1967), High-Pressure Recnnaissance investigations in the system Mg_2SiO_4-H_2O, *Earth Planet. Sci. Lett.*, *2*, 130–133.
Rivers, M., V. B. Prakapenka, A. Kubo, C. Pullins, C. M. Holl, and S. D. Jacobsen (2008), The COMPRES/GSECARS gas-loading system for diamond anvil cells at the Advanced Photon Source, *High Pressure Res.*, *28*, 273–292.
Saal, A. E., E. H. Hauri, M. Lo Cascio, J. A. Van Orman, M. C. Rutherford, and R. F. Cooper (2008), Volatile content of lunar volcanic glasses and the presence of water in the Moon's interior, *Nature*, *454*, 192–196.
Sawamoto, H., D. J. Weidner, S. Sasaki, and M. Kumazawa (1984), Single-crystal elastic properties of the modified spinel (beta) phase of magnesium orthosilicate, *Science*, *224*, 749–751.
Schmerr, N., and E. Garnero (2007), Upper mantle discontinuity topography from thermal and chemical heterogeneity, *Science*, *318*, 623–626.
Sinogeikin, S. V., T. Katsura, and J. D. Bass (1998), Sound velocities and elastic properties of Fe-bearing wadsleyite and ringwoodite, *J. Geophys. Res.*, *103*, 20,819–20,825, doi:10.1029/98JB01819.
Sinogeikin, S. V., J. D. Bass, and T. Katsura (2003), Single-crystal elasticity of ringwoodite high pressures and high temperature: Implications for 520 km seismic discontinuty, *Phys. Earth Planet. Int.*, *136*, 41–66.
Smyth, J. R. (1987), β-Mg_2SiO_4: A potential host for water in the mantle?, *Am. Mineral.*, *72*, 1051–1055.
Smyth, J. R. (1994), A Crystallographic model for hydrous wadsleyite (β-Mg_2SiO_4): An ocean in the Earth's interior, *Am. Mineral.*, *79*, 1021–1024.
Smyth, J. R., T. Kawamoto, S. D. Jacobsen, J. R. Swope, R. L. Hervig, and J. R. Holloway (1997), Crystal structure of monoclinic hydrous wadsleyite [β-$(Mg,Fe)_2SiO_4$], *Am. Mineral.*, *82*, 270–275.

Speziale, S., C.-S. Zha, T. S. Duffy, R. J. Hemley, and H.-K. Mao (2001), Quasi-hydrostatic compression of magnesium oxide to 52 GPa: Implications for the pressure-volume-temperature equation of state, *J. Geophys. Res.*, *106*, 515–528, doi:10.1029/2000JB900318.

Stixrude, L., and C. Lithgow-Bertelloni (2005), Thermodynamics of mantle minerals: 1. Physical properties, *Geophys. J. Int.*, *162*, 610–632.

Tange, Y., Y. Nishihara, and T. Tsuchiya (2009), Unified analyses for P-V-T equation of state of MgO: A solution for pressure-scale problems in high P-T experiments, *J. Geophys. Res.*, *114*, B03208, doi:10.1029/2008JB005813.

Thomas, S.-M., S. D. Jacobsen, C. R. Bina, P. Reichart, M. Moser, E. H. Hauri, M. Koch-Müller, J. R. Smyth, and G. Dollinger (2015), Quantification of water in hydrous ringwoodite, *Front. Earth. Sci.*, *2*, doi:10.3389/feart.2014.00038.

Tian, L., J. Zhao, W. Liu, L. Liu, H. Liu, and J. Du (2012), Effect of iron on high pressure elasticity of hydrous wadsleyite and ringwoodite by first-principles simulation, *High Pressure Res.*, *32*(3), 385–395.

Tsuchiya, J., and T. Tsuchiya (2009), First principles investigation of the structural and elastic properties of hydrous wadsleyite under pressure, *J. Geophys. Res.*, *114*, B02206, doi:10.1029/2008JB005841.

Wang, J., J. D. Bass, and T. Kastura (2014), Elastic properties of iron-bearing wadsleyite to 17.7 GPa: Implications for mantle models, *Phys. Earth Planet. Int.*, *228*, 92–96.

Wu, Z., R. M. Wentzcovitch, K. Umemoto, B. Li, K. Hirose, and J. C. Zheng (2008), Pressure-volume-temperature relations in MgO: An ultrahigh pressure-temperature scale for planetary sciences applications, *J. Geophys. Res.*, *113*, B06204, doi:10.1029/2009JB000828.

Ye, Y., R. A. Schwering, and J. R. Smyth (2009), Effects of hydration on thermal expansion of forsterite, wadsleyite, and ringwoodite at ambient pressure, *Am. Mineral.*, *94*, 899–904.

Ye, Y., J. R. Smyth, A. Hushur, M. H. Manghnani, D. Lonappan, P. Dera, and D. J. Frost (2010), Crystal structure of hydrous wadsleyite with 2.8% H_2O and compressibility to 60 GPa, *Am. Mineral.*, *95*, 1765–1772.

Yusa, H., and T. Inoue (1997), Compressibility of hydrous wadsleyite (β-phase) in Mg_2SiO_4 by high pressure X-ray diffraction, *Geophys. Res. Lett.*, *24*(14), 1831–1834, doi:10.1029/97GL51794.

Zha, C. S., T. S. Duffy, H.-K. Mao, R. T. Downs, R. J. Hemley, and D. J. Weidner (1997), Single-crystal elasticity of beta-Mg_2SiO_4 to the pressure of the 410 km seismic discontinuity in the Earth's mantle, *Earth Planet. Sci. Lett.*, *147*, E9–E15.

Zha, C. S., T. S. Duffy, R. T. Downs, H.-K. Mao, and R. J. Hemley (1998), Brillouin scattering and X-ray diffraction of San Carlos olivine: Direct pressure determination to 32 GPa, *Earth Planet. Sci. Lett.*, *159*, 25–33.

Zha, C. S., H.-K. Mao, and R. J. Hemley (2000), Elasticity of MgO and a primary pressure scale to 55 GPa, *Proc. Natl. Acad. Sci. U.S.A.*, *97*, 13,494–13,499.